Growth-limiting role of endothelial cells in endoderm development.

Wolfhagen Sand, Fredrik; Hörnblad, Andreas; Johansson, Jenny; Lorén, Christina; Edsbagge, Josefina; Ståhlberg, Anders; Magenheim, Judith; Ilovich, Ohad; Mishani, Eyal; Dor, Yuval; Ahlgren, Ulf; Semb, Henrik

Published in:
Developmental Biology

DOI:
10.1016/j.ydbio.2011.01.026

2011

Growth-limiting role of endothelial cells in endoderm development

Fredrik Wolfhagen Sand[a], Andreas Hörnblad[b,1], Jenny K. Johansson[a,1], Christina Lorén[b,1], Josefina Edsbagge[c], Anders Ståhlberg[a,d], Judith Magenheim[e], Ohad Ilovich[f], Eyal Mishani[f], Yuval Dor[e], Ulf Ahlgren[b] and Henrik Semb[a,2]

[a] Stem Cell and Pancreas Developmental Biology, Stem Cell Center, Department of Laboratory Medicine, Lund ,Lund University, BMC B10, Klinikgatan 26, SE-221 84 Lund, Sweden

[b] Umeå Centre for Molecular Medicine, Umeå University, SE-901 87 Umeå, Sweden

[c] Cellartis AB, Arvid Wallgrens Backe 20, SE-413 46 Göteborg, Sweden

[d] Present address: Lundberg Laboratory for Cancer Research, Department of Pathology, Sahlgrenska Academy at University of Gothenburg, Gula Stråket 8, SE-413 45 Göteborg, Sweden

[e] Department of Developmental Biology and Cancer Research, The Institute for Medical Research Israel-Canada, The Hebrew University-Hadassah Medical School, Jerusalem 91120, Israel

[f] Department of Nuclear Medicine, Cyclotron Unit, Hadassah Hebrew University Hospital, Jerusalem, Israel

[1] These authors contributed equally to the study

[2] Author for correspondence: Henrik Semb

Stem cell center

Department of Laboratory Medicine, Lund

Lund University

BMC, B10

SE: 221 84 Lund, Sweden

Telephone: +46-46-2223159

Fax: +46-46-2223600

E-mail: henrik.semb@med.lu.se

Key words: Pancreas, endoderm, morphogenesis, blood vessel, mesenchyme, sphingosine-1-phosphate 1 receptor

Abstract

Endoderm development is dependent on inductive signals from different structures in close vicinity, including the notochord, lateral plate mesoderm and endothelial cells. Recently, we demonstrated that a functional vascular system is necessary for proper pancreas development, and that sphingosine-1-phosphate (S1P) exhibits the traits of a blood vessel-derived molecule involved in early pancreas morphogenesis. To examine whether $S1P_1$-signaling plays a more general role in endoderm development, *$S1P_1$*-deficient mice were analyzed. $S1P_1$ ablation results in compromised growth of several foregut-derived organs, including the stomach, dorsal and ventral pancreas and liver. Within the developing pancreas the reduction in organ size was due to deficient proliferation of $Pdx1^+$ pancreatic progenitors, whereas endocrine cell differentiation was unaffected. Ablation of endothelial cells in vitro did not mimic the $S1P_1$ phenotype, instead, increased organ size and hyperbranching were observed. Consistent with a negative role for endothelial cells in endoderm organ expansion, excessive vasculature was discovered in $S1P_1$-deficient embryos. Altogether, our results show that endothelial cell hyperplasia negatively influences organ development in several foregut-derived organs.

Introduction

Organ and vascular development are interdependent processes where cross talk between blood vessels and the developing organ anlagen regulates proper organ architecture and function. In the present investigation the effect of a perturbed vascular system on development of foregut-derived organs was studied in *sphingosine-1-phosphate receptor 1* (*$S1P_1$*) deficient embryos. $S1P_1$ is a G-coupled receptor and is the founding member of a family of five receptors, $S1P_{1-5}$, formerly known as EDG receptors. $S1P_1$'s ligand, sphingosine-1-phosphate (S1P), is a bioactive lipid found at high concentrations in the blood stream where it binds to albumin and high density lipoprotein (HDL). Blood-born S1P is produced and secreted by red blood cells, platelets, monocytes, mast cells, and possibly endothelial cells (Pappu et al., 2007; Venkataraman et al., 2008; Yatomi et al., 1995). In the surrounding tissues S1P is found at lower levels due to degradation by S1P lyase (Schwab et al., 2005). The conserved and ubiquitously expressed enzymes sphingosine kinase 1 (SphK1) and 2 synthesize S1P by phosphorylation of sphingosine (Spiegel and Milstien, 2002). Upon receptor binding S1P mediates cell proliferation (Zhang et al., 1991), survival (Paris et al., 2002), migration (Sadahira et al., 1992), and morphogenesis (Kupperman et al., 2000). $S1P_{1-3}$ are widely expressed whereas $S1P_4$ is expressed in lymphoid tissues and $S1P_5$ in the central nervous system and spleen. $S1P_{1-3}$ play critical roles in vascular maturation. For example, ablating $S1P_1$ in mice results in massive hemorrhages and destabilization of blood vessels causing lethality before E14.5 (Kono et al., 2004; Liu et al., 2000).

The definitive endoderm gives rise to a number of organs along the primitive gut tube, including the pharynx, thyroid, parathyroid, esophagus, lungs, thymus, stomach, liver, pancreas, small and large intestine. Endoderm development involves axis formation, induction, expansion and differentiation/maturation. Signals from mesodermally-derived tissues in close vicinity to the endoderm, such as the notochord, heart, splanchnic

mesenchyme and endothelium, control many aspects of these processes (Deutsch et al., 2001; Golosow and Grobstein, 1962; Hebrok et al., 1998; Kim et al., 1997; Lammert et al., 2001; Wessells and Cohen, 1967; Yoshitomi and Zaret, 2004).

Reciprocal signaling between the splanchnic mesenchyme and the endoderm mediates the induction of several organ primordia along the anterior-posterior axis of the gut tube. Furthermore, mesenchyme to endoderm signaling, via FGF10, plays a central role in the proliferation of progenitors within the thyroid, thymus, lung, liver, pancreas, stomach and caecum (Berg et al., 2007; Bhushan et al., 2001; Burns et al., 2004; Min et al., 1998; Nyeng et al., 2007; Ohuchi et al., 2000; Revest et al., 2001; Sekine et al., 1999). These observations were recently supported by genetic evidence, demonstrating that failure to form the dorsal pancreatic mesenchyme in Isl1-, N-cadherin- and Raldh2-ablated embryos results in dorsal pancreatic agenesis (Ahlgren et al., 1997; Esni et al., 2001; Martin et al., 2005).

Endothelial cells influence liver development already when the hepatic cells infiltrate the septum transversum before vascular function (Matsumoto et al., 2001). Furthermore, increased liver vasculature results in hyperplasia of the liver due to paracrine factors (LeCouter et al., 2003). In vitro culturing of lung rudiments under hypoxic conditions leads to augmented vessel density and reduced lung epithelial branching. Moreover, over expression of VEGF A in vivo results in increased vascular density and reduced branching of the lung epithelium (Akeson et al., 2003; Zeng et al., 1998). During pancreas development initiation of the dorsal pancreatic bud, maintenance of expression of the crucial pancreatic and duodenal homeobox 1 (Pdx1) transcription factor, induction of the pancreas specific transcription factor 1a (Ptf1a) and endocrine cell specification also depend on endothelial signals (Lammert et al., 2001; Yoshitomi and Zaret, 2004). In contrast, endothelial cells are not necessary for similar events in the ventral bud (Yoshitomi and Zaret, 2004). Endoderm-endothelial interactions continue after the mesenchyme is infiltrated by blood vessels. For example, over expression

of VEGF A under the control of the Pdx1 promoter expands the endocrine compartment, whereas the acinar compartment is reduced, suggesting that endocrine and exocrine cell differentiation is controlled by the vasculature. Taken together these data clearly illustrate the importance of well-balanced interactions between the mesenchyme and endothelium with the endoderm for proper induction and expansion of gut-derived organs.

The vasculature signals both via endothelial cells and its content. Recently, we have showed that a functional vascular system plays an important role in dorsal pancreas development by supplying signaling cues from the circulation, and in particular through, S1P (Edsbagge et al., 2005).

To directly address the functional role of S1P signaling within endothelial cells during endoderm development, *$S1P_1$* deficient embryos were analyzed. Here, we demonstrate that $S1P_1$, which is specifically expressed in the endothelium, is required for growth of several foregut derivatives, including stomach, dorsal and ventral pancreas, and liver. We also show that growth of the pancreatic endoderm requires $S1P_1$ function, and that reduction in pancreatic volume is caused by a decrease in progenitor proliferation. However, endocrine cell differentiation was unaffected. We were also able to reproduce these results in vitro, thereby excluding indirect effects via changes in the supply of oxygen and nutrients. Surprisingly, endothelial cell ablation failed to mimic the $S1P_1$ phenotype. Instead, increased pancreatic organ size and hyper branching were observed. Together with the observation of increased number of endothelial cells in $S1P_1$-deficient embryos, these results point towards a hitherto unknown concept of endothelial cells limit expansion of foregut-derived organs.

Results

$S1P_1$ is expressed in endothelial cells during embryogenesis

To determine the $S1P_1$ protein expression profile in the developing endoderm, triple immunofluorescence labeling of E-cadherin (Ecad), $S1P_1$ and Pecam was conducted. $S1P_1$ specifically co-localized with Pecam in endothelial cells at E9.5 and E12.5 (Fig. 1 and S1). During early stages (E9.5) the gut endoderm is primarily exposed to endothelial cells in the form of the dorsal aorta (Fig. 1A), whereas the various endoderm-derived organ anlagen later interacts with endothelial cells within the surrounding splanchnic mesenchyme (Fig. 1B-E). $S1P_1$ expression was also detected in the central nervous system, but not within the endoderm (Fig. 1 and data not shown).

Growth of foregut-derived organ primordia is compromised in $S1P_1$-deficient embryos

To determine the functional role of $S1P_1$ during foregut endoderm development, the epithelial volume of various foregut-derived organ anlagen was measured using Optical Projection Tomography (OPT). Consistent with the original observation, *$S1P_1$*-deficient embryos died before E14.5 due to cardiovascular defects (Liu et al., 2000). Although the size of the embryos was not severely affected at E12.5, hemorrhages within the central nervous system and the limb buds were observed (Fig. 2A-B). Several of the foregut-derived organs were affected in the $S1P_1$ mutants (Fig. 2C-D). Besides, the expression levels of Ecad increased along the anterior-posterior axis of the foregut endoderm. For example, Ecad expression was higher in the pancreas compared to in the lung (Fig. 2C-D). The difference in expression levels of Ecad might be due to the fact that lung is a much more branched and tubular organ at this time point, compared to the pancreas. OPT analysis demonstrated that the dorsal (Fig. 2K-M) and ventral (Fig. 2N-P) pancreas and the stomach (Fig. 2H-J) were significantly reduced in size in *$S1P_1$*-/- embryos. The dorsal pancreas was, on average, reduced by 32%, the ventral pancreas by 45% and the stomach by 32%. As a result, the protrusion of the *$S1P_1$*-/-

dorsal pancreatic bud was reduced (Fig. 2C-D). The lung (Fig. 2E-G, and data not shown) showed a similar trend in size reduction (30%) together with a decline in distal tip number. However, these changes were not statistically significant. For liver volume analyses the high endogenous autofluorescence precluded the use of E-cadherin stainings. Instead, OPT measurements of the liver volumes are based on endogenous autofluorescence and demonstrated a 61% reduction (Fig. 2Q-S). For an overview of all the organs included in the data set see Supplementary Figure S2 A-B.

To address if $S1P_1$ ablation resulted in morphological changes in the surrounding endodermal mesenchyme, a cutting plane was placed in the autofluorescence channel with the Ecad channel being kept intact. This analysis revealed no dramatic changes in the organization of the mesenchyme surrounding the dorsal pancreas (Fig. 2T-U and supplementary video 1-2).

To investigate the onset of perturbed expansion of pancreatic endoderm in *$S1P_1$* -/- embryos, quantification of the dorsal pancreatic volume was conducted by whole mount E-cadherin stainings. Whereas no difference in the size of the dorsal pancreas was found at E10.5 (Fig. 3A-C), at E11.5 a 23% reduction was observed in $S1P_1$ mutants, compared to controls (Fig. 3D-F).

The functional role of $S1P_1$ in expansion of the pancreatic endoderm is independent of circulatory factors

To further resolve how *$S1P_1$* may control expansion of foregut endoderm derivatives, we focused on one particular foregut-derived organ, i.e. the pancreas. To eliminate the possibility that the endodermal phenotype observed in *$S1P_1$*-deficient embryos was caused by defective circulation, development of the pancreatic endoderm was studied in vitro. At E11.5, no obvious morphological or embryo survival differences were observed between *$S1P_1$* -/- embryos and their litter mate controls (insets in Fig. 4A-B) (Liu et al., 2000). However,

although control explants consistently developed normally (27 out of 30), the phenotype of the *S1P$_1$* -/- explants was rather diverse, spanning from severely compromised growth to merely a reduction in size and degree of branching (Fig. 4A-C and S3A-F). In fact, a high percentage (25 %) of the S1P$_1$-deficient explants did not grow at all (Fig. 4C). Even when the more naïve pancreatic endoderm was analyzed in vitro similar observations were made. Specifically, analysis of E9.5 *S1P$_1$* mutant explants cultured in vitro for 4 days (corresponding to E11.5-12.5 in vivo), revealed aberrant development of the pancreatic endoderm (Fig. 4D-F).

S1P$_1$ is required for proliferation of Pdx1$^+$ pancreatic progenitors but dispensable for endocrine differentiation.

To test if the observed defective growth of the epithelium involved changes in cell proliferation, sections from E12.5 BrdU-pulsed embryos were stained for Pdx1 and BrdU. Proliferating cells were observed in both the pancreatic mesenchyme and epithelium, in both genotypes (Fig. 5A-B). However, the proliferative rate of Pdx1$^+$ cells was significantly lower in *S1P$_1$*-deficient embryos compared to their littermate control embryos (Fig. 5C).
Caspase 3 staining of E12.5 dorsal pancreas revealed insignificant apoptotic activities in control and *S1P$_1$*-deficient embryos, thus excluding apoptosis as an explanation for how S1P$_1$ signaling controls pancreatic endoderm expansion (Fig. S4). To examine whether necrosis increased in *S1P$_1$*-deficient embryos, expression of the inflammatory marker CD45 was investigated since an increase in CD45$^+$ cells within the epithelium would indicate ongoing inflammation and necrosis. However, no increase in the relative number of CD45$^+$ cells was found (Fig S4). Altogether, these data suggests that reduced cell proliferation, but not an increase in apoptosis or necrosis, explains the reduced organ size in *S1P$_1$*-deficient embryos.

At E12.5, glucagon$^+$ cells are the most abundant hormone-producing cell type in the dorsal pancreas. To investigate if endocrine differentiation relies on $S1P_1$ function, whole mount staining of the dorsal pancreatic bud for Ecad and glucagon were conducted (Fig. 5D). At E12.5, $S1P_1$ deficiency resulted in no significant change in alpha cell differentiation compared to the littermate controls (Fig. 5E). Notably, confocal measurements of the epithelial volume matched our OPT findings (Fig. 5F). To address if beta cell differentiation was affected, E11.5 explants were cultured for two days and analyzed by whole mount staining using insulin and E-cadherin antibodies (Fig. 5G). Consistent with the in vivo analysis, in vitro culture of the dorsal pancreas resulted in reduced volume of the mutant dorsal pancreas (Fig. 5I). However, $S1P_1$ deficiency resulted in no significant change in the relative number of insulin$^+$ cells (5H). QPCR analysis of E12.5 dorsal pancreatic buds was in line with these observations, which demonstrated that *Ngn3, Pax4* and *6, Pdx1* and *insulin* mRNA expression was unchanged in $S1P_1$ mutants (Fig. 5K-O).

QPCR analysis of the markers for various progenitor populations, including *Cpa1* (tip cells at E12.5 and later acinar cells) (Zhou et al., 2007), *Sox9* (multipotent progenitors at E12.5 and later ducts) (Seymour et al., 2007) as well as the acinar marker *amylase* revealed, no statistical change in the relative mRNA expression (Fig. 5P-R). Furthermore, an analysis of the distribution of the lumenal marker, Mucin1, revealed that the overall luminal network in the *$S1P_1$* -/- dorsal bud was comparable to the controls (Fig. 5J). However, the proximal part of the *$S1P_1$* -/- pancreatic duct was slightly less branched, which probably is secondary to the overall reduction in organ size.

Thus, $S1P_1$ is required for proliferation of the Pdx1$^+$ pancreatic progenitors, but not for early endocrine and exocrine cell specification.

Gene expression analysis of the E10.5 $S1P_1$ -/- dorsal pancreas

To mechanistically dissect the role of $S1P_1$ in pancreas development we first examined the mRNA expression levels of genes known to control endoderm development. Ptf1a controls dorsal pancreas specification and is expressed in multipotent progenitors but later becomes restricted to acinar cells (Krapp et al., 1996; Yoshitomi and Zaret, 2004). $S1P_1$ ablation resulted in no change in the mRNA and protein expression of *Ptf1a* (Fig. 6A, H-O), neither was there a change in the mRNA expression of two mesenchymal markers known to play functional roles during pancreatic development, *Isl1* (Ahlgren et al., 1997) and *Wilms tumor 1 homolog (Wt1)* (Wagner et al., 2005)(Fig. 6B-C). Consistent with the above, protein levels of Isl-1, which is also expressed in endocrine progenitors, were unaffected in $S1P_1$ mutant pancreatic endoderm and mesenchyme (Fig. 6P-Q). We also analyzed the expression of FGF ligand/receptor family members known to control expansion of the pancreatic epithelium via mesenchyme-to-epithelium signaling (Bhushan et al., 2001; Dichmann et al., 2003; Elghazi et al., 2002; Miralles et al., 1999). However, expression of *FGF10* (*FGF7* could not be detected in all samples and was therefore excluded) and its receptor *FGFR2* were unaffected upon $S1P_1$ ablation (Fig. 6D-E). Finally, the mRNA expression of two other *S1P* receptors, $S1P_{2\text{-}3}$, which are present in the developing pancreatic mesenchyme, showed no compensatory effect on the mRNA expression of these receptors was observed (Fig. 6F-G).

Blood vessel ablation results in increased pancreatic organ size

Our initial hypothesis evolved around the assumption that endothelial cells, via $S1P_1$, provide inductive signals necessary for expansion of the pancreatic endoderm. To directly address this hypothesis, we ablated endothelial cells in vitro using 1-[4-(6,7-Dimethoxy-quinolin-4-yloxy)-3-fluoro-phenyl]-3-(2-fluoro-phenyl)-urea (Ilovich et al., 2008), hereafter referred to as quinolin-urea, and examined the consequences on pancreatic endoderm development. Two days treatment with the quinolin-urea resulted in total ablation of the blood vessels (visualized

by Pecam1) (Fig. 7A-B). Surprisingly, efficient ablation of endothelial cells at E11.5 did not result in compromised expansion of the epithelium, instead, increased organ size and hyperbranching of the pancreatic endoderm were observed (Fig. 7A-B). Both the ventral and dorsal buds were affected, but the effect was most striking on the ventral bud (Fig. 7C-D).

$S1P_1$ ablation results in increased vascular density in foregut-derived organ anlagen

The endothelial cell ablation results contradicted our initial hypothesis and instead suggested that endothelial cells may limit the growth of foregut-derived organs. Thus, a possible mechanism for how $S1P_1$ ablation may reduce endoderm organ expansion could involve hypervascularization. Indeed, previous studies demonstrated increased vascular density in the developing *$S1P_1$* -/- limb bud (Chae et al., 2004). Consistent with this observation, we found that $S1P_1$ ablation results in hypervascularization (2-3-fold increase in blood vessel density) within the mesenchyme surrounding the foregut-derived organs, including the dorsal pancreas (Fig. 8A-C), lung (Fig. 8D-F), stomach (Fig. 8G-I) and liver (Fig. 8J-L).

Discussion

Blood vessels are essential for the developing organism because they provide oxygen and nutrients as well as inductive cues that control cell proliferation and cell fate specification during organogenesis. For example, blood vessels communicate with the surrounding tissue in the developing retina and this interplay controls both differentiation and proliferation of blood vessels and the surrounding astrocytes (West et al., 2005). Furthermore, endothelial cells control the development of endoderm-derived organs, e.g. both liver and dorsal pancreas outgrowth and early pancreatic endocrine cell specification (Lammert et al., 2001; Yoshitomi and Zaret, 2004). However, questions that remain include the identity and nature of these endothelial signals, and whether they exclusively act in a positive manner or play a more dynamic role by also negatively affecting endoderm development. In this study we present evidence in support of endothelial cells playing a hitherto unknown general role in foregut-derived organ development by limiting growth.

Initially, the analysis of *S1P$_1$* -/- mice, which show destabilized blood vessels and hemorrhages (Liu et al., 2000), revealed a reduction in organ size of the foregut-derived organs, including lung, liver, stomach and pancreas. We specifically investigated the role of this pathway in early pancreas development and now demonstrate that S1P$_1$ ablation results in reduced size of the dorsal and ventral pancreatic buds, but that it has no effect on endocrine or exocrine cell fate specification. The dorsal pancreatic bud size reduction is due to a decrease in proliferation rate of Pdx1$^+$ progenitors, indicating that S1P$_1$ is required for proliferation, but not differentiation, of Pdx1$^+$ pancreatic progenitors. The in vivo findings were reproduced in vitro, implying that these findings do not represent indirect effects due to the circulation phenotype of *S1P$_1$* embryos.

To verify that the requirement of S1P$_1$ for pancreatic endoderm expansion is mediated by endothelial cells, which is the only cell type within the developing pancreas where S1P$_1$

protein can be detected, blood vessels were ablated at E11.5 in wild type gut/pancreatic explants. Unexpectedly, removing blood vessels did not mimic the $S1P_1$ phenotype. Instead, blood vessel ablation resulted in pancreatic endoderm expansion and hyperbranching, suggesting that endothelial cells limit expansion of the pancreatic epithelium. The blood vessel ablator, quinolin-urea, inhibits VEGFR2 and PDGFRβ (Ilovich et al., 2008) which are expressed by the blood vessels in the pancreas (Lammert et al., 2001). PDGFRβ is additionally also expressed in the pancreatic mesenchyme (Hori et al., 2008). As neither of the receptors are expressed in the pancreatic epithelium, this excludes a direct effect of the quinolin-urea on the epithelium through these receptors. The fact that blood vessel ablation failed to mimic the $S1P_1$ phenotype suggested that $S1P_1$ is not directly involved in the reduced growth of foregut-derived organs. Alternatively, the $S1P_1$ phenotype may be secondarily caused by an increase in blood vessel density. In fact, this hypothesis is in line with previous work demonstrating that $S1P_1$-deficiency results in hypervascularization in the limb bud (Chae et al., 2004). Consistent with this, we show that $S1P_1$ ablation results in increased number of blood vessels in the mesenchyme that surrounds the foregut-derived organs, including the pancreas, stomach, liver and lung. Altogether, these observations provide evidence (both gain-of-function and loss-of-function) in support of a model where endothelial cells counteract growth-promoting signals – potentially mesenchyme-derived – by providing growth-limiting signals to the pancreatic endoderm. Endothelial cell ablation experiments will have to confirm whether the same model applies to the other foregut-derived organs as well. Previously, the consequence of increased vascularization during pancreas development has been studied by expressing VEGF under control of the Pdx1 promoter. The over growth of blood vessels resulted in an increase (three fold) in endocrine mass and a dramatic decrease (seven fold) in acinar mass (Lammert et al., 2001). Although the consequence of $S1P_1$ deficiency also involves hypervascularization, no effect on early endocrine or exocrine cell

differentiation was observed. However, the early lethality of $S1P_1$ mutant animals permitted the analysis of differentiation no later than E12.5. This is at the brink of secondary transition when the variation in endocrine differentiation between embryos is substantial, which might therefore, mask any difference. It is also possible that two opposing mechanisms act in parallel in the $S1P_1$ deficient pancreas, i.e. a pro-endocrine effect mediated by the elevated blood vessel density and a negative effect on endocrine differentiation by the hypoxia caused by defective blood vessels (Chae et al., 2004; Heinis et al.). Notably, the decrease in the $Pdx1^+$ progenitor pool in $S1P_1$ -/- mice is consistent with the observed reduction in acinar cells in adult Pdx1-VEGF mice (Lammert et al., 2001). Endothelial cells also play a functional role during the earlier stages of pancreas development by initiating dorsal pancreas formation via Ptf1a induction (Jacquemin et al., 2006; Yoshitomi and Zaret, 2004).

In the lung, manipulation of blood vessel development has highlighted the need for proper control of density, and spatio- temporal distribution of the blood vessels (Akeson et al., 2003; Schwarz et al., 2000; van Tuyl et al., 2005; Zeng et al., 1998). Taken together it is obvious that the balance between blood vessel growth and organ growth must be tightly controlled. In a previous study it has been shown that induced hypervascularization during adulthood results in liver hyperplasia (LeCouter et al., 2003). Hypervascularization during embryogenesis, in the $S1P_1$ mutants, results in hypoplasia of the liver. A possible explanation for these contrary findings could be that different mechanisms are involved during adulthood and embryogenesis. The influence of the blood vessels on the surrounding tissue might also be different during different phases of development.

It is well established that the development of foregut-derived organs, such as the pancreas, lung, stomach and liver, rely on signals from mesenchymal and endothelial cells (Fukuda and Yasugi, 2005; Gittes, 2009; Shannon and Hyatt, 2004; Warburton et al., 2000; Zaret, 2002; Zaret, 2008). However, whether endothelial cell signals play a more general role in

development of endoderm-derived organs has so far remained unknown. Our results show that endothelial cell hyperplasia negatively influences organ development in several foregut-derived organs, including the pancreas, stomach, lung and liver, suggesting that endothelial cells counterbalance growth stimulatory signals originating from other cells, such as mesenchymal cells (for a schematic illustration see Figure S3A-C). In the lung and stomach, blood vessels are mainly located within the mesenchyme without direct contact with the epithelium, whereas in the liver and pancreas, the blood vessels are located within both the mesenchyme and the epithelium. It is therefore probable that the molecule, which negatively influences endodermal growth, is a blood vessel-derived diffusible molecule or an extracellular matrix component. Future studies will be necessary to clarify the identity and mechanism of action of the endothelial cell-derived molecule(s) regulating organogenesis of foregut-derived organs.

Materials and Methods

Animals

$S1P_1$-deficient mice were back-crossed for at least 10 generations into C57BL6. Endoderm development was indistinguishable between wild type and SIP_1 +/- mice. Genotyping of *$S1P_1$* mice was performed as previously described but with small modifications as (Liu et al., 2000). The mice were housed in the animal facilities at the Lund Biomedical Center, Lund University, Sweden, kept according to animal care guidelines and all experimental procedures were approved by the regional animal ethic committee, Lund and Malmö, Sweden.

Immunofluorescence and immunoreagents

For immunofluorescence, embryos, explants and whole mounts were fixed, sectioned and stained as previously described (Ahnfelt-Ronne et al., 2007; Edsbagge et al., 2005; Esni et al., 2001; Esni et al., 1999). Antibodies used were guinea pig anti Pdx1, 1:1000 (kind gift from Chris Wright); rat anti Ecad, 1:400 (ECCD-2, Takara); mouse anti Ecad, 1:100 (BD Biosciences); rat anti Pecam-1 (CD31), 1:100 (BD Pharmingen); goat anti Pecam-1 (CD31), 1:500 (R&D Systems); rabbit anti $S1P_1$, 1:500 (Santa Cruz Biotechnology); Armenian hamster anti Mucin1, 1:500 (Thermo Fischer Scientific); rabbit anti Ptf1a 1:2500 (BCBC, www.betacell.org/), guinea pig anti glucagon 1:500 (Linco), guinea pig anti insulin 1:800 (Linco), rat anti CD45 1:100 (Abcam) and rabbit anti Isl-1 1:100 (Chemicon). Nuclear staining was performed with 4',6-diamidino-2-phenylindole (DAPI). Proliferating cells were detected with rat anti-BrdU, 1:200 (Nordic BioSite) 50 mg/kg BrdU was injected intraperitoneally 2 hours (h) before the pregnant female was sacrificed. Apoptosis was detected with rabbit anti Caspase 3, 1:1000 (R&D Systems). Secondary antibodies used were from Molecular Probes and Jackson Immuno Research Laboratory Inc. Specimens (sections, whole mounts and cultured pancreatic rudiments) were analyzed using a Zeiss Axioplan

microscope and an Apotome unit or a Zeiss LSM 510 confocal microscope. The images were processed using Adobe Photoshop and Imaris. Blood vessel density quantification was performed on sections throughout the entire organ (separated by at least 50 μM) which were stained with Pecam and E-Cadherin antibodies and DAPI. Axiovision's feather automatic measurement was used. Total blood vessel area for respective organ was divided by total organ area – total epithelial area.

Optical Projection Tomography analysis

E12.5 isolated respiratory- and gastrointestinal tracts were fixed in 4% PFA for 1h at 4^{o}C. Fixed tissues were washed in PBS, stepwise dehydrated into Methanol and stored in -20^{o}C until used. Before staining the tissues were rehydrated into TBST (0.15 M NaCl, 0.1M Tris pH 7.5, 0.1% Triton X-100) and thoroughly washed. The specimen were blocked in blocking solution (TBST, 10% normal goat serum (Cedar Lane Lab) and 0.01% Sodium azide (Sigma S-8032) for 24h at RT, incubated with primary antibody in blocking solution for 24h at RT and washed extensively for 24 in TBST. Incubation with secondary antibody was performed as with primary antibody. The secondary antibody solution was filtered through an Acrodisc syringe filter (Pall life sciences, 0,45 μm) to avoid precipitate induced artifacts during OPT scanning. Tissues were washed in TBST for 24h and prepared for OPT scanning as previously described (Alanentalo et al., 2007). Antibodies used were: Rat anti Ecad (clone ECCD-2, Zymed) at 1:500 dilution and Alexa 594 goat anti rat (Molecular Probes) at 1:500. For the liver, endogenous autofluorescence was used to define the organ.

The specimen were scanned through 360^{o} using the Bioptonics 3001 OPT scanner (Bioptonics) modified with an exciter D560/40X and emitter E610lpv2 filter (Chroma) for optimal visualization of Alexa 594 fluorescence. All samples were scanned at the same

magnification. Tomographic sections (resolution: 1024x1024) of the samples were generated using the NRecon V1.5.0 (SkyScan) software. Orthogonal planes were assessed using DataViewer V1.3.2 (SkyScan). Volume renderings and isosurfaces were created using Volocity v5.3.1 (Improvision, Coventry, United Kingdom). Quantification of organ epithelial volumes, based on the Ecad signal, was performed using the quantification software module for Volocity v5.3.1. The original image stacks of GI tract epithelium were manually cropped into lung, stomach, ventral pancreas and dorsal pancreas. A "find objects by intensity" task was applied to select voxels according to a specified intensity threshold value. The value was chosen to exclude pixels not contributing the labeled objects (the organ epithelium). A fine filter (3×3 kernel) was also applied to the data sets to avoid selection of background noise voxels with intensities above the threshold level. The volumes of the measured objects were finally exported to the Excel 2007 (Microsoft Corporation, Redmond, Washington) software for statistical analysis.

Culture of pancreatic rudiments

Isolation, recombination, and culture of pancreatic rudiments were carried out essentially as previously described (Ahlgren et al., 1996; Esni et al., 2001; Gittes and Galante, 1993). The explants were cultured from 48h up to six days in a humidified incubator of 37°C with 5% CO_2. Only *S1P$_1$*-deficient embryos of similar size as their wild type littermates with no apparent external morphological changes, except for shorter limbs and tail and hemorrhages, were chosen for analysis. For the blood vessel ablation experiments, quinolin-urea was added to the culture medium (0,5 µM) at day one of culture.

Quantitative real-time PCR

Dorsal buds from E10.5 or E12.5 embryos were dissected and directly frozen in lysis buffer. Total RNA was extracted with QIAshredder together with RNeasy Micro Kit (Qiagen) according to the manufactures' instructions. Reverse transcription was performed in 10 µL reactions with SuperScript III (Invitrogen) according to the manufacturer's instruction using a mixture of 2.5 µM oligo(dT) and random hexamers (Invitrogen). All samples were diluted to 200 µL with water prior to real-time PCR. Real-time PCR measurements were performed on a LightCycler 480 (Roche Diagnostics). 10 µL reactions contained 10 mM Tris (pH 8.3), 50 mM KCl, 3 mM $MgCl_2$, 0.3 mM dNTP, 1 U JumpStart Taq Polymerase (all Sigma-Aldrich), 0.25 X SYBR Green I (Invitrogen), 400 nM of each primer (Invitrogen) and 2 µL cDNA. Primer sequences are available as supplementary data (Fig. S5). Actb and B2m were measured using primers contained in the Mouse Endogenous Control Panel supplied by TATAA Biocenter. All samples were run as duplicates. Formation of expected PCR products was confirmed by agarose gel electrophoresis and melting curve analysis for all samples. Gene expression data was normalized against the geometric average of Actb and B2m and data analysis was performed as described (Nolan et al., 2006; Stahlberg et al., 2008).
For E12.5 samples StepOnePLUS Real Time PCR system from Applied Biosystems was used. The samples were normalized against HPRT and not run in duplicates.

References

Ahlgren, U., Jonsson, J., Edlund, H., 1996. The morphogenesis of the pancreatic mesenchyme is uncoupled from that of the pancreatic epithelium in IPF1/PDX1-deficient mice. Development. 122**,** 1409-16.

Ahlgren, U., Pfaff, S. L., Jessell, T. M., Edlund, T., Edlund, H., 1997. Independent requirement for ISL1 in formation of pancreatic mesenchyme and islet cells. Nature. 385**,** 257-60.

Ahnfelt-Ronne, J., Jorgensen, M. C., Hald, J., Madsen, O. D., Serup, P., Hecksher-Sorensen, J., 2007. An improved method for three-dimensional reconstruction of protein expression patterns in intact mouse and chicken embryos and organs. J Histochem Cytochem. 55**,** 925-30.

Akeson, A. L., Greenberg, J. M., Cameron, J. E., Thompson, F. Y., Brooks, S. K., Wiginton, D., Whitsett, J. A., 2003. Temporal and spatial regulation of VEGF-A controls vascular patterning in the embryonic lung. Dev Biol. 264**,** 443-55.

Alanentalo, T., Asayesh, A., Morrison, H., Loren, C. E., Holmberg, D., Sharpe, J., Ahlgren, U., 2007. Tomographic molecular imaging and 3D quantification within adult mouse organs. Nat Methods. 4**,** 31-3.

Berg, T., Rountree, C. B., Lee, L., Estrada, J., Sala, F. G., Choe, A., Veltmaat, J. M., De Langhe, S., Lee, R., Tsukamoto, H., Crooks, G. M., Bellusci, S., Wang, K. S., 2007. Fibroblast growth factor 10 is critical for liver growth during embryogenesis and controls hepatoblast survival via beta-catenin activation. Hepatology. 46**,** 1187-97.

Bhushan, A., Itoh, N., Kato, S., Thiery, J. P., Czernichow, P., Bellusci, S., Scharfmann, R., 2001. Fgf10 is essential for maintaining the proliferative capacity of epithelial progenitor cells during early pancreatic organogenesis. Development. 128**,** 5109-17.

Burns, R. C., Fairbanks, T. J., Sala, F., De Langhe, S., Mailleux, A., Thiery, J. P., Dickson, C., Itoh, N., Warburton, D., Anderson, K. D., Bellusci, S., 2004. Requirement for fibroblast growth factor 10 or fibroblast growth factor receptor 2-IIIb signaling for cecal development in mouse. Dev Biol. 265**,** 61-74.

Chae, S. S., Paik, J. H., Allende, M. L., Proia, R. L., Hla, T., 2004. Regulation of limb development by the sphingosine 1-phosphate receptor S1p1/EDG-1 occurs via the hypoxia/VEGF axis. Dev Biol. 268**,** 441-7.

Deutsch, G., Jung, J., Zheng, M., Lora, J., Zaret, K. S., 2001. A bipotential precursor population for pancreas and liver within the embryonic endoderm. Development. 128**,** 871-81.

Dichmann, D. S., Miller, C. P., Jensen, J., Scott Heller, R., Serup, P., 2003. Expression and misexpression of members of the FGF and TGFbeta families of growth factors in the developing mouse pancreas. Dev Dyn. 226**,** 663-74.

Edsbagge, J., Johansson, J. K., Esni, F., Luo, Y., Radice, G. L., Semb, H., 2005. Vascular function and sphingosine-1-phosphate regulate development of the dorsal pancreatic mesenchyme. Development. 132**,** 1085-92.

Elghazi, L., Cras-Meneur, C., Czernichow, P., Scharfmann, R., 2002. Role for FGFR2IIIb-mediated signals in controlling pancreatic endocrine progenitor cell proliferation. Proc Natl Acad Sci U S A. 99**,** 3884-9.

Esni, F., Johansson, B. R., Radice, G. L., Semb, H., 2001. Dorsal pancreas agenesis in N-cadherin- deficient mice. Dev Biol. 238**,** 202-12.

Esni, F., Taljedal, I. B., Perl, A. K., Cremer, H., Christofori, G., Semb, H., 1999. Neural cell adhesion molecule (N-CAM) is required for cell type segregation and normal ultrastructure in pancreatic islets. J Cell Biol. 144**,** 325-37.

Fukuda, K., Yasugi, S., 2005. The molecular mechanisms of stomach development in vertebrates. Dev Growth Differ. 47**,** 375-82.
Gittes, G. K., 2009. Developmental biology of the pancreas: a comprehensive review. Dev Biol. 326**,** 4-35.
Gittes, G. K., Galante, P. E., 1993. A culture system for the study of pancreatic organogenesis J. Tissue Cult. Methods. Volume 15**,** 23-27.
Golosow, N., Grobstein, C., 1962. Epitheliomesenchymal interaction in pancreatic morphogenesis. Dev Biol. 4**,** 242-55.
Hebrok, M., Kim, S. K., Melton, D. A., 1998. Notochord repression of endodermal Sonic hedgehog permits pancreas development. Genes Dev. 12**,** 1705-13.
Heinis, M., Simon, M. T., Ilc, K., Mazure, N. M., Pouyssegur, J., Scharfmann, R., Duvillie, B., Oxygen tension regulates pancreatic beta-cell differentiation through hypoxia-inducible factor 1alpha. Diabetes. 59**,** 662-9.
Hori, Y., Fukumoto, M., Kuroda, Y., 2008. Enrichment of putative pancreatic progenitor cells from mice by sorting for prominin1 (CD133) and platelet-derived growth factor receptor beta. Stem Cells. 26**,** 2912-20.
Ilovich, O., Jacobson, O., Aviv, Y., Litchi, A., Chisin, R., Mishani, E., 2008. Formation of fluorine-18 labeled diaryl ureas--labeled VEGFR-2/PDGFR dual inhibitors as molecular imaging agents for angiogenesis. Bioorganic & Medicinal Chemistry. 16**,** 4242-4251.
Jacquemin, P., Yoshitomi, H., Kashima, Y., Rousseau, G. G., Lemaigre, F. P., Zaret, K. S., 2006. An endothelial-mesenchymal relay pathway regulates early phases of pancreas development. Dev Biol. 290**,** 189-99.
Kim, S. K., Hebrok, M., Melton, D. A., 1997. Notochord to endoderm signaling is required for pancreas development. Development. 124**,** 4243-52.
Kono, M., Mi, Y., Liu, Y., Sasaki, T., Allende, M. L., Wu, Y. P., Yamashita, T., Proia, R. L., 2004. The sphingosine-1-phosphate receptors S1P1, S1P2, and S1P3 function coordinately during embryonic angiogenesis. J Biol Chem. 279**,** 29367-73.
Krapp, A., Knofler, M., Frutiger, S., Hughes, G. J., Hagenbuchle, O., Wellauer, P. K., 1996. The p48 DNA-binding subunit of transcription factor PTF1 is a new exocrine pancreas-specific basic helix-loop-helix protein. EMBO J. 15**,** 4317-29.
Kupperman, E., An, S., Osborne, N., Waldron, S., Stainier, D. Y., 2000. A sphingosine-1-phosphate receptor regulates cell migration during vertebrate heart development. Nature. 406**,** 192-5.
Lammert, E., Cleaver, O., Melton, D., 2001. Induction of pancreatic differentiation by signals from blood vessels. Science. 294**,** 564-7.
LeCouter, J., Moritz, D. R., Li, B., Phillips, G. L., Liang, X. H., Gerber, H. P., Hillan, K. J., Ferrara, N., 2003. Angiogenesis-independent endothelial protection of liver: role of VEGFR-1. Science. 299**,** 890-3.
Liu, Y., Wada, R., Yamashita, T., Mi, Y., Deng, C. X., Hobson, J. P., Rosenfeldt, H. M., Nava, V. E., Chae, S. S., Lee, M. J., Liu, C. H., Hla, T., Spiegel, S., Proia, R. L., 2000. Edg-1, the G protein-coupled receptor for sphingosine-1-phosphate, is essential for vascular maturation. J Clin Invest. 106**,** 951-61.
Martin, M., Gallego-Llamas, J., Ribes, V., Kedinger, M., Niederreither, K., Chambon, P., Dolle, P., Gradwohl, G., 2005. Dorsal pancreas agenesis in retinoic acid-deficient Raldh2 mutant mice. Dev Biol. 284**,** 399-411.
Matsumoto, K., Yoshitomi, H., Rossant, J., Zaret, K. S., 2001. Liver organogenesis promoted by endothelial cells prior to vascular function. Science. 294**,** 559-63.
Min, H., Danilenko, D. M., Scully, S. A., Bolon, B., Ring, B. D., Tarpley, J. E., DeRose, M., Simonet, W. S., 1998. Fgf-10 is required for both limb and lung development and

exhibits striking functional similarity to Drosophila branchless. Genes Dev. 12**,** 3156-61.
Miralles, F., Czernichow, P., Ozaki, K., Itoh, N., Scharfmann, R., 1999. Signaling through fibroblast growth factor receptor 2b plays a key role in the development of the exocrine pancreas. Proc Natl Acad Sci U S A. 96**,** 6267-72.
Nolan, T., Hands, R. E., Bustin, S. A., 2006. Quantification of mRNA using real-time RT-PCR. Nat Protoc. 1**,** 1559-82.
Nyeng, P., Norgaard, G. A., Kobberup, S., Jensen, J., 2007. FGF10 signaling controls stomach morphogenesis. Dev Biol. 303**,** 295-310.
Ohuchi, H., Hori, Y., Yamasaki, M., Harada, H., Sekine, K., Kato, S., Itoh, N., 2000. FGF10 acts as a major ligand for FGF receptor 2 IIIb in mouse multi-organ development. Biochem Biophys Res Commun. 277**,** 643-9.
Pappu, R., Schwab, S. R., Cornelissen, I., Pereira, J. P., Regard, J. B., Xu, Y., Camerer, E., Zheng, Y. W., Huang, Y., Cyster, J. G., Coughlin, S. R., 2007. Promotion of lymphocyte egress into blood and lymph by distinct sources of sphingosine-1-phosphate. Science. 316**,** 295-8.
Paris, F., Perez, G. I., Fuks, Z., Haimovitz-Friedman, A., Nguyen, H., Bose, M., Ilagan, A., Hunt, P. A., Morgan, W. F., Tilly, J. L., Kolesnick, R., 2002. Sphingosine 1-phosphate preserves fertility in irradiated female mice without propagating genomic damage in offspring. Nat Med. 8**,** 901-2.
Revest, J. M., Suniara, R. K., Kerr, K., Owen, J. J., Dickson, C., 2001. Development of the thymus requires signaling through the fibroblast growth factor receptor R2-IIIb. J Immunol. 167**,** 1954-61.
Sadahira, Y., Ruan, F., Hakomori, S., Igarashi, Y., 1992. Sphingosine 1-phosphate, a specific endogenous signaling molecule controlling cell motility and tumor cell invasiveness. Proc Natl Acad Sci U S A. 89**,** 9686-90.
Schwab, S. R., Pereira, J. P., Matloubian, M., Xu, Y., Huang, Y., Cyster, J. G., 2005. Lymphocyte sequestration through S1P lyase inhibition and disruption of S1P gradients. Science. 309**,** 1735-9.
Schwarz, M. A., Zhang, F., Gebb, S., Starnes, V., Warburton, D., 2000. Endothelial monocyte activating polypeptide II inhibits lung neovascularization and airway epithelial morphogenesis. Mech Dev. 95**,** 123-32.
Sekine, K., Ohuchi, H., Fujiwara, M., Yamasaki, M., Yoshizawa, T., Sato, T., Yagishita, N., Matsui, D., Koga, Y., Itoh, N., Kato, S., 1999. Fgf10 is essential for limb and lung formation. Nat Genet. 21**,** 138-41.
Seymour, P. A., Freude, K. K., Tran, M. N., Mayes, E. E., Jensen, J., Kist, R., Scherer, G., Sander, M., 2007. SOX9 is required for maintenance of the pancreatic progenitor cell pool. Proc Natl Acad Sci U S A. 104**,** 1865-70.
Shannon, J. M., Hyatt, B. A., 2004. Epithelial-mesenchymal interactions in the developing lung. Annu Rev Physiol. 66**,** 625-45.
Spiegel, S., Milstien, S., 2002. Sphingosine 1-phosphate, a key cell signaling molecule. J Biol Chem. 277**,** 25851-4.
Stahlberg, A., Elbing, K., Andrade-Garda, J. M., Sjogreen, B., Forootan, A., Kubista, M., 2008. Multiway real-time PCR gene expression profiling in yeast Saccharomyces cerevisiae reveals altered transcriptional response of ADH-genes to glucose stimuli. BMC Genomics. 9**,** 170.
Wagner, N., Wagner, K. D., Theres, H., Englert, C., Schedl, A., Scholz, H., 2005. Coronary vessel development requires activation of the TrkB neurotrophin receptor by the Wilms' tumor transcription factor Wt1. Genes Dev. 19**,** 2631-42.

van Tuyl, M., Liu, J., Wang, J., Kuliszewski, M., Tibboel, D., Post, M., 2005. Role of oxygen and vascular development in epithelial branching morphogenesis of the developing mouse lung. Am J Physiol Lung Cell Mol Physiol. 288**,** L167-78.

Warburton, D., Schwarz, M., Tefft, D., Flores-Delgado, G., Anderson, K. D., Cardoso, W. V., 2000. The molecular basis of lung morphogenesis. Mech Dev. 92**,** 55-81.

Venkataraman, K., Lee, Y. M., Michaud, J., Thangada, S., Ai, Y., Bonkovsky, H. L., Parikh, N. S., Habrukowich, C., Hla, T., 2008. Vascular endothelium as a contributor of plasma sphingosine 1-phosphate. Circ Res. 102**,** 669-76.

Wessells, N. K., Cohen, J. H., 1967. Early pancreas organogenesis: Morphogenesis, tissue interactions, and mass effects. Developmental Biology. 15**,** 237-270.

West, H., Richardson, W. D., Fruttiger, M., 2005. Stabilization of the retinal vascular network by reciprocal feedback between blood vessels and astrocytes. Development. 132**,** 1855-62.

Yatomi, Y., Ruan, F., Hakomori, S., Igarashi, Y., 1995. Sphingosine-1-phosphate: a platelet-activating sphingolipid released from agonist-stimulated human platelets. Blood. 86**,** 193-202.

Yoshitomi, H., Zaret, K. S., 2004. Endothelial cell interactions initiate dorsal pancreas development by selectively inducing the transcription factor Ptf1a. Development. 131**,** 807-17.

Zaret, K. S., 2002. Regulatory phases of early liver development: paradigms of organogenesis. Nat Rev Genet. 3**,** 499-512.

Zaret, K. S., 2008. Genetic programming of liver and pancreas progenitors: lessons for stem-cell differentiation. Nat Rev Genet. 9**,** 329-40.

Zeng, X., Wert, S. E., Federici, R., Peters, K. G., Whitsett, J. A., 1998. VEGF enhances pulmonary vasculogenesis and disrupts lung morphogenesis in vivo. Dev Dyn. 211**,** 215-27.

Zhang, H., Desai, N. N., Olivera, A., Seki, T., Brooker, G., Spiegel, S., 1991. Sphingosine-1-phosphate, a novel lipid, involved in cellular proliferation. J Cell Biol. 114**,** 155-67.

Zhou, Q., Law, A. C., Rajagopal, J., Anderson, W. J., Gray, P. A., Melton, D. A., 2007. A multipotent progenitor domain guides pancreatic organogenesis. Dev Cell. 13**,** 103-14.

During the revision process two relevant papers have been published:

Pierreux, C. E., Cordi, S., Hick, A. C., Achouri, Y., Ruiz de Almodovar, C., Prevot, P. P., Courtoy, P. J., Carmeliet, P., Lemaigre, F. P., Epithelial: Endothelial cross-talk regulates exocrine differentiation in developing pancreas. Dev Biol. 347**,** 216-27.

Shah, S. R., Esni, F., Jakub, A., Paredes, J., Lath, N., Malek, M., Potoka, D. A., Prasadan, K., Mastroberardino, P. G., Shiota, C., Guo, P., Miller, K. A., Hackam, D. J., Burns, R. C., Tulachan, S. S., Gittes, G. K., Embryonic mouse blood flow and oxygen correlate with early pancreatic differentiation. Dev Biol.

Acknowledgments

We thank Dr. R. Proia for providing the $S1P_1$ deficient mouse line and for valuable comments on the manuscript, Dr. K. Gaengel and Dr. C. Betsholtz for constructive discussions and for sharing unpublished data, Dr. C. Wright and BCBC for providing antibodies, Dr. I. Artner for valuable comments on the manuscript, M. Magnusson and C. Ekenstierna for mouse breeding. This work was supported by the Swedish Research Council, Stem Cell Center, Lund University, Swedish Foundation for Strategic Research, NIH Beta Cell Biology Consortium, Juvenile Diabetes Research Foundation, and in part by the Intramural Research Program of the National Institutes of Health, National Institute of Diabetes and Digestive and Kidney Diseases, The Kempe Foundations, The Swedish Medical Research Council and Umeå University Biotech Grants.

Figures and Tables

Figure 1 $S1P_1$ is expressed by endothelial cells within the mesenchyme.

Immunofluorescence was used to investigate $S1P_1$ expression within the embryonic primitive gut tube and its later derived organs. $S1P_1$ (red), co-expressed with Pecam1 positive blood vessels (blue). The endoderm is visualized by Ecad (green). The inset in (A) shows Pdx1 (red) in the part of the endoderm (green), which represent the dorsal pancreas. Throughout the early phase of endodermal development $S1P_1$ expression can be detected in blood vessels, neural ectoderm and blood cells. Between E9 and E12 the dorsal pancreas is separated from the $S1P_1^+$ dorsal aorta by the invading mesenchyme. The mesenchyme is infiltrated by $S1P_1^+$ blood vessels that reestablish the endoderm-endothelial interaction (C). E12.5 $S1P_1$ expressing blood vessels are found in the mesenchyme surrounding both the lung (E) and stomach (B) epithelium as well as in the blood vessels of the liver (D). Dorsal pancreas (dp), dorsal aorta (da). Scale bars 100 µm.

Figure 2 Quantification of endoderm volumes at E12.5. The *$S1P_1$* deficient embryos suffer from hemorrhages in the central nervous system and in the shortened extremities (A-B). As reported earlier the overall size of the embryos was not severely affected at E12.5. Several foregut-derived organs were affected by *$S1P_1$* ablation (C-D). The dorsal pancreatic bud from *$S1P_1$* deficient embryos protrudes shorter from the duodenum compared to littermate controls (C-D). Note the difference in Ecad intensity between the endoderm organs, with intense Ecad signal in the pancreatic buds, whereas less signal was detected within the lungs. The volume of the endoderm organs; lung, dorsal and ventral pancreas and stomach from *$S1P_1$* deficient embryos were quantified using OPT (E-P). The volume of the *$S1P_1$* deficient dorsal (32%) and ventral (45%) pancreata and stomach (32%), as analyzed by OPT, is significantly reduced compared to the littermate controls (M, P, J), whereas the lung was reduced by 30% but did

not reach significance (G). All images are isosurface renderings based on the signal from E-cadherin stainings. The volume of the liver was quantified using OPT based on endogenous autofluorescence (Q-S). The liver volume was reduced by 61 % (S). In order to investigate if *S1P$_1$* ablation resulted in morphological changes in the mesenchyme surrounding the endoderm, a cutting plane was placed in the autofluorescence channel whereas the Ecad channel was keep intact. This analysis revealed no dramatic change in the organization of the mesenchyme surrounding the dorsal pancreas (T-U). Scale bars are 100 µm in all except A-D and Q-R where they are 500 µm. In G, J, M, P and S *S1P$_1$* -/- is compared to *S1P$_1$* +/+ and +/- with student T-test. Lung comparison, p=0,0989, Dorsal bud comparison, p=0,0296, ventral comparison, p=0,0334, stomach comparison, p=0,0239 and liver comparison, p=0,0003. Error bars represent ± SEM. *S1P$_1$* -/- n=6 and *S1P$_1$* +/- n=8. Lu=lung, Es=esophagus, St=stomach, Dp=dorsal pancreas, Vp=ventral pancreas and Du=duodenum.

Figure 3 The *S1P$_1$* endodermal phenotype is detectable at E11.5. To investigate how early the *S1P$_1$* endodermal phenotype could be detected dorsal pancreatic volume were measured after confocal analysis. E11.5 a reduction of the mutants dorsal pancreatic volume by 23% could be detected (D-F) but not at E10.5 (A-C). Dp=dorsal pancreas and Vp=ventral pancreas. Scale bars 100 µm.

Figure 4 In vitro culture of E9.5 and E11.5 *S1P$_1$*-deficient pancreatic explants fails to rescue the phenotype. To confirm the reduced growth seen in vivo cultures of E11.5 explanted gut tubes were carried out in vitro. Immunofluorescence analysis of the epithelial marker Ecad (red) concluded that in vitro culture of *S1P$_1$* deficient explants is not sufficient to rescue the pancreatic phenotype (A-C), as insets in A and B the embryos are shown. *S1P$_1$* +/+ littermate controls n=8, +/- n=22, and -/- n=12. To verify that the endoderm had not been

permanently damage already at E11.5, E9.5 cultures were also carried out, Ecad (red) and Pdx1 (green). Even though the success rate in littermate controls were slightly lower, the *S1P$_1$* mutant explants developed notably worse (D-F). *S1P$_1$* +/+ littermate controls n=3, +/- n=5, and -/- n=6. These data support the hypothesis that the phenotype is not just secondary to the cardio-vascular phenotype. Scale bars 100 µm. The explants showed in A-B are also included in the volume quantification in Figure 5H.

Figure 5 Proliferation of Pdx1$^+$ progenitors is reduced but endocrine differentiation is unaffected in the *S1P$_1$* -/- dorsal pancreas. Proliferation within the Pdx1$^+$ epithelium was analyzed by immunofluorescence of in utero BrdU pulsed embryos. Proliferating cells marked with BrdU (green), were found both inside the Pdx1$^+$ epithelium (red), and outside in the mesenchyme in both *S1P$_1$* deficient embryos and littermate controls (A-B). BrdU$^+$ cells in the epithelium are indicated with filled arrowheads and in the mesenchyme indicated with open arrowheads. Scale bar 100 µm. Proliferation of Pdx1$^+$ progenitors was significantly reduced (35%) (student T-test) in the *S1P$_1$* deficient dorsal pancreas (littermate controls n=7, *S1P$_1$* deficient embryos n=5, p =0,0049) red and black dots represents different litters (C). To investigate if alpha cell differentiation was affected, glucagon and Ecad volumes of the dorsal bud were estimated by confocal microscopy. No difference between *S1P$_1$* deficient embryos and littermate controls could be detected in glucagon volume divided by Ecad volume (student T-test, p=0,2188) (E). Note the variation within the littermate control group. Consistent with the OPT analysis a statistically significant decrease in the volume of the *S1P$_1$* deficient dorsal pancreatic epithelium was detected with confocal microscopy (student T-test, p=0,0014) (F). Each color of the dots represents a different litter (littermate controls n=10, *S1P$_1$* deficient embryos n=9). Representative samples are shown in D, Ecad (grey) and glucagon (green). Note the unevenly distribution of the endocrine cells which are

concentrated to the tip of the bud. Scale bar 100 µm. To analyze beta cell differentiation, the relative number of insulin$^+$ cell (insulin volume divided by Ecad volume) was estimated in E11.5 explants cultured for two days. No difference in the relative number of insulin$^+$ cells in *S1P$_1$* deficient embryos and littermate controls was detected (student T-test, p=0,2587) (H). Consistently, a statistically significant reduction of the dorsal pancreatic epithelium volume was observed (student T-test, p=0,0014) (I). Littermate controls n=6, *S1P$_1$* deficient embryos n=4. Representative samples are shown in G, Ecad (grey) and insulin (green). In *S1P$_1$* deficient embryos ductal organization as visualized by Mucin1 staining (red) was unaffected (J). Further analysis of cell differentiation was carried out by QPCR measurements. Expression levels of *Ngn3* (K), *Pax4* (L), *Pax6* (M), *Pdx1* (N), *insulin* (O), *Sox9* (P), *Cpa1* (Q) and *amylase* (R) were measured but no statistical differences were detected. P-values; *ngn3* p=0,5503, *Pax4* p=3012, *Pax6* p=0,6057, *Pdx1* p=1456, *insulin* p=0,0645, *Sox9* p=0,8861, *Cpa1* p=0,4472 and *amylase* p=0,1380.

Figure 6 Marker expression analysis of the *S1P$_1$*-deficient pancreas. QPCR was used to analyze mRNA expression of genes known to be involved in development of the endoderm; *Ptf1a* (A) which is known to be induced by blood vessels, as well as the mesenchymal genes *Isl1* (B) and *Wt1* (C) were quantified. We could not detect any statistical difference in any of these genes. The FGF pathway including *FGF10* (D) and its receptor *FGFR2* (E) known to be important for the expansion many of the endodermal organs and significantly for the pancreatic progenitors were measured. In none of these genes we could detect different expression levels between *S1P$_1$* deficient dorsal pancreata and littermate controls. To investigate if *S1P$_1$* deficient dorsal pancreata had an upregulation of the two other pancreatic expressed family members *S1P$_2$* (F) and *S1P$_3$* (G) we used QPCR to analyze the relative expression levels. For *S1P$_2$* and *S1P$_3$* no upregulation was detected. *S1P$_1$* +/+ littermate

controls n=5, +/- littermate controls n=11, and $S1P_1$ -/- embryos n=4. Student T-test was used; error bars represent standard error of the mean.

To verify the mRNA data whole mount immunofluorescence labeling of Ecad (green), Ptf1a (red) and Pdx1 (grey) was used. Whole mount immunofluorescence labeling did not reveal any altered expression levels of Ptf1a in E10.5 embryos (H-O). Neither did protein expression analysis of Isl1 and Pdx1 on E10.5 pancreatic sections (P-Q). Scale bars 100 µm.

Figure 7 Blood vessel ablation does not mimic the *S1P$_1$* phenotype, but results in expansion and hyperbranching of the pancreatic epithelium. Blood vessel ablation did not mimic the phenotype seen in *S1P$_1$*-deficient explants (A-D). Total ablation of Pecam1 (red) positive blood vessels was seen after two days of treatment with quinolin-urea (Qu). The epithelium was visualized by Ecad (grey) (A-B). The epithelium was also analyzed using the luminal marker Mucin1 (red). Both dorsal and ventral pancreas is affected by the blood vessel ablation, but the hyperbrancing effect is most prominent in the ventral pancreas (C-D). Dp=dorsal pancreas and Vp=ventral pancreas. Scale bars 100 µm

Figure 8 *S1P$_1$* ablation results in hypervascularization. In all the investigated endodermal organs *S1P$_1$* ablation resulted in increased vascular density (A-B, D-E, G-H and I-J). The epithelium is visualized by Ecad (green) and the blood vessels by Pecam (red). For clarity, the liver is shown both without Ecad and in insets with Ecad (I-J). Scale bar 100 µm. The blood vessel density was quantified by measuring the blood vessel area and dividing it with the total area of the organ – the epithelial area (C, F and I). Due to the endogenous autofluorescence of the liver we used QPCR to quantify the blood vessel marker *Pecam* (K). In all organs we found a 2-3-fold increase in blood vessel density. P values; pancreas p= 0,0184, littermate controls n=3, and *S1P$_1$* -/- embryos n=4, stomach p=0,006, littermate controls n=3, and *S1P$_1$* -

/- embryos n=4, lung p=0,0019, littermate controls n=3, and *S1P$_1$* -/- embryos n=3 and liver p=0,0214, littermate controls n=9, and S1P$_1$ -/- embryos n=5. d. pancreas=dorsal pancreas. Scale bar 100 µm.

Figure S1 Same images as in Figure 1 but with each cannel shown individually. S1P$_1$ (red) co-localizes with Pecam (blue) positive blood vessels, the epithelium is marked with E-cadherin (green). Dorsal pancreas (dp or d. pancreas), dorsal aorta (da). Scale bars 100 µm.

Figure S2 Overview of the data set from the volume quantification at E12.5. OPT isosurface renderings of all samples used in volume quantifications at E12.5 are presented in (A) stomach, lung, ventral pancreas (Vp) and dorsal pancreas (Dp) and in (B) liver. Wt=wild type, Het=heterozygote and Ko=knockout. Scale bars in A 100 µm and in B 500 µm.

Figure S3 Overview of the E11.5 explants. The *S1P$_1$* mutant explants spanned from merely a reduction in size reduction and branching (A) to severely compromised growth (B-C). Small variations in the growth of the controls were observed (D-F). Scale bars 100 µm.

Figure S4 Neither apoptosis nor necrosis explain the reduced organ size in *S1P$_1$* ablated embryos. Cleaved Caspase-3 was used to investigate apoptosis. E13.5 limb buds were used as a positive control, note the positive staining between the digits (A). Apoptotic cells were found in the pancreatic mesenchyme and rarely in the epithelium (B). The numbers of positive cells were extremely few and could not explain the reduction of pancreatic organ size seen in the *S1P$_1$* mutants. To address if necrosis could be an alternative explanation, the presence of CD45$^+$ inflammatory cells was analyzed. The adult spleen and pancreas were used as controls

(C). $CD45^+$ cells were numerous in the adult spleen, but rare in the adult pancreas. In the E12.5 dorsal pancreas, the presence of $CD45^+$ cells was unaffected by *$S1P_1$* ablation (D).

Figure S5 QPCR primer sequences.

Figure S6 Model of how growth control in the developing pancreatic endoderm. Schematic illustration of growth control in the wild type, blood vessel ablated and *$S1P_1$*-deficient pancreas. In the wild type pancreas positive signals from the mesenchyme (yellow), such as FGFs, are counterbalanced by negative signals from blood vessels (red) (A). When blood vessels are ablated in vitro the negative signals from the blood vessels are lost, allowing massive expansion and hyperbranching of the epithelium (blue) (B). In the opposite scenario, as in the *$S1P_1$*-deficient embryos, hypervascularization results in increased negative signals from the blood vessels. As a consequence epithelial proliferation decreases leading to compromised growth of the epithelium (C).

Supplementary video 1 Overview of mesenchyme and isosurface renderings based on the signal from E-cadherin staining showing stomach, ventral and dorsal pancreas from a wild type specimen.

Supplementary video 2 Overview of mesenchyme and isosurface renderings based on the signal from E-cadherin staining showing stomach, ventral and dorsal pancreas from a *$S1P_1$* deficient specimen.

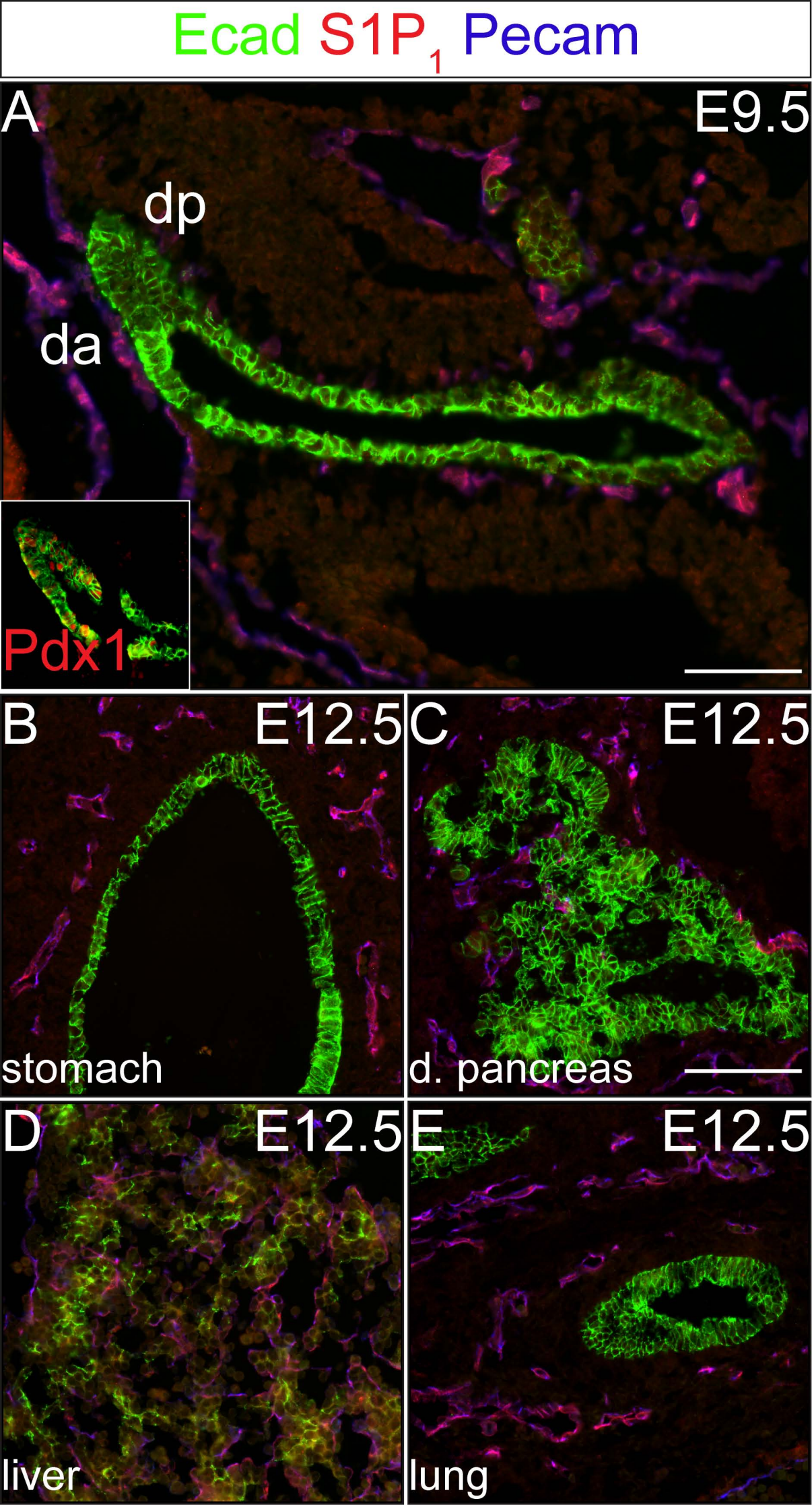
Ecad S1P1 Pecam
A
E9.5
dp
da
Pdx1
B
E12.5
stomach
C
E12.5
d. pancreas
D
E12.5
liver
E
E12.5
lung

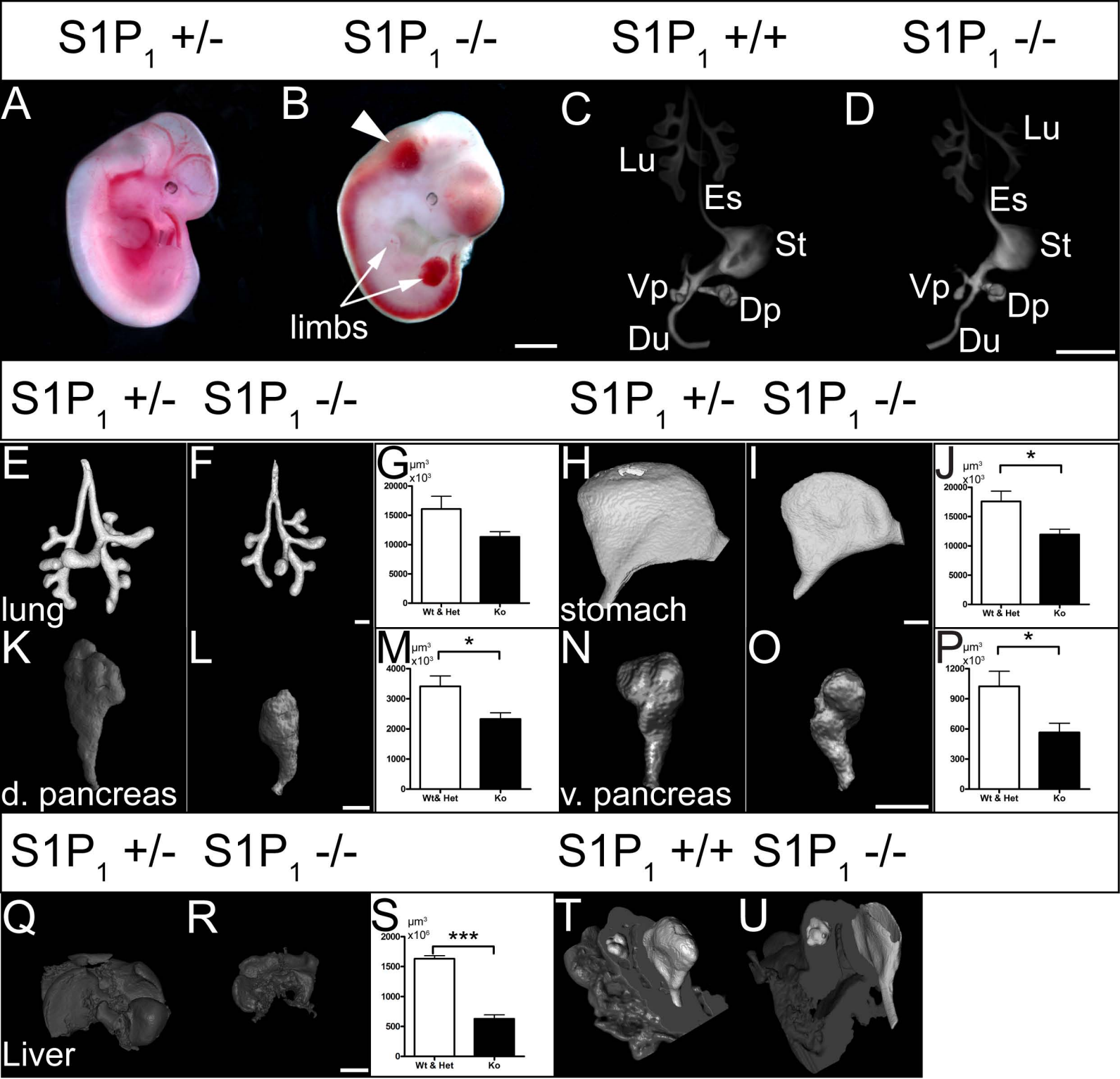
S1P1 +/-
S1P1 -/-
S1P1 +/+
S1P1 -/-
A
B
limbs
C
Lu
Es
St
Vp
Dp
Du
D
Lu
Es
St
Vp
Dp
Du
S1P1 +/- S1P1 -/-
S1P1 +/- S1P1 -/-
E
lung
F
G
µm3 x10³
20000
15000
10000
5000
0
Wt & Het
Ko
H
stomach
I
J
µm3 x10³
*
20000
15000
10000
5000
0
Wt & Het
Ko
K
d. pancreas
L
M
µm3 x10³
*
4000
3000
2000
1000
0
Wt& Het
Ko
N
v. pancreas
O
P
µm3 x10³
*
1200
900
600
300
0
Wt & Het
Ko
S1P1 +/- S1P1 -/-
S1P1 +/+ S1P1 -/-
Q
Liver
R
S
µm3 x10⁶
***
2000
1500
1000
500
0
Wt & Het
Ko
T
U

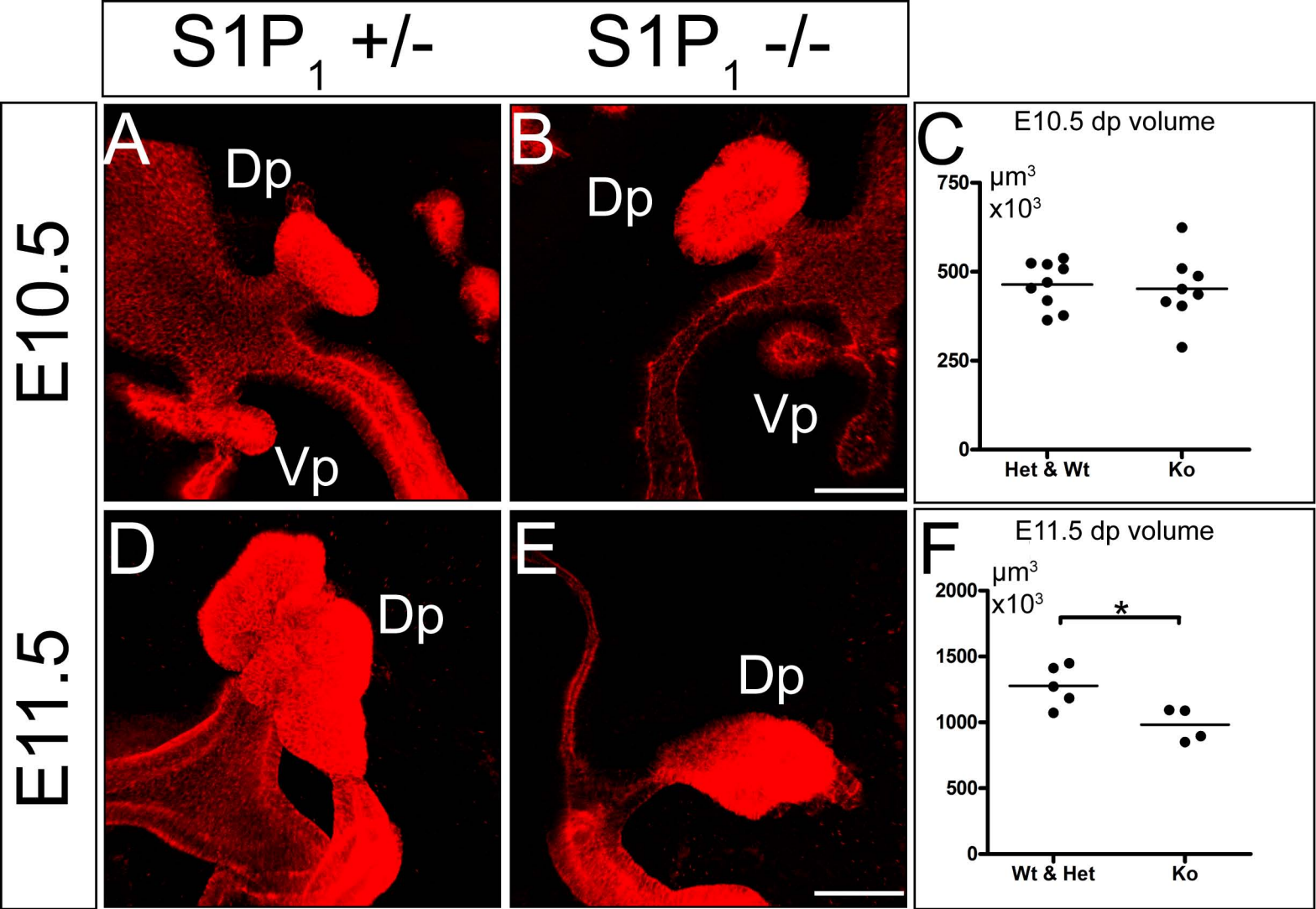
S1P1 +/-
S1P1 -/-
E10.5
E11.5
A
Dp
Vp
B
Dp
Vp
C
E10.5 dp volume
µm3
x103
750
500
250
0
Het & Wt
Ko
D
Dp
E
Dp
F
E11.5 dp volume
µm3
x103
2000
1500
1000
500
0
*
Wt & Het
Ko

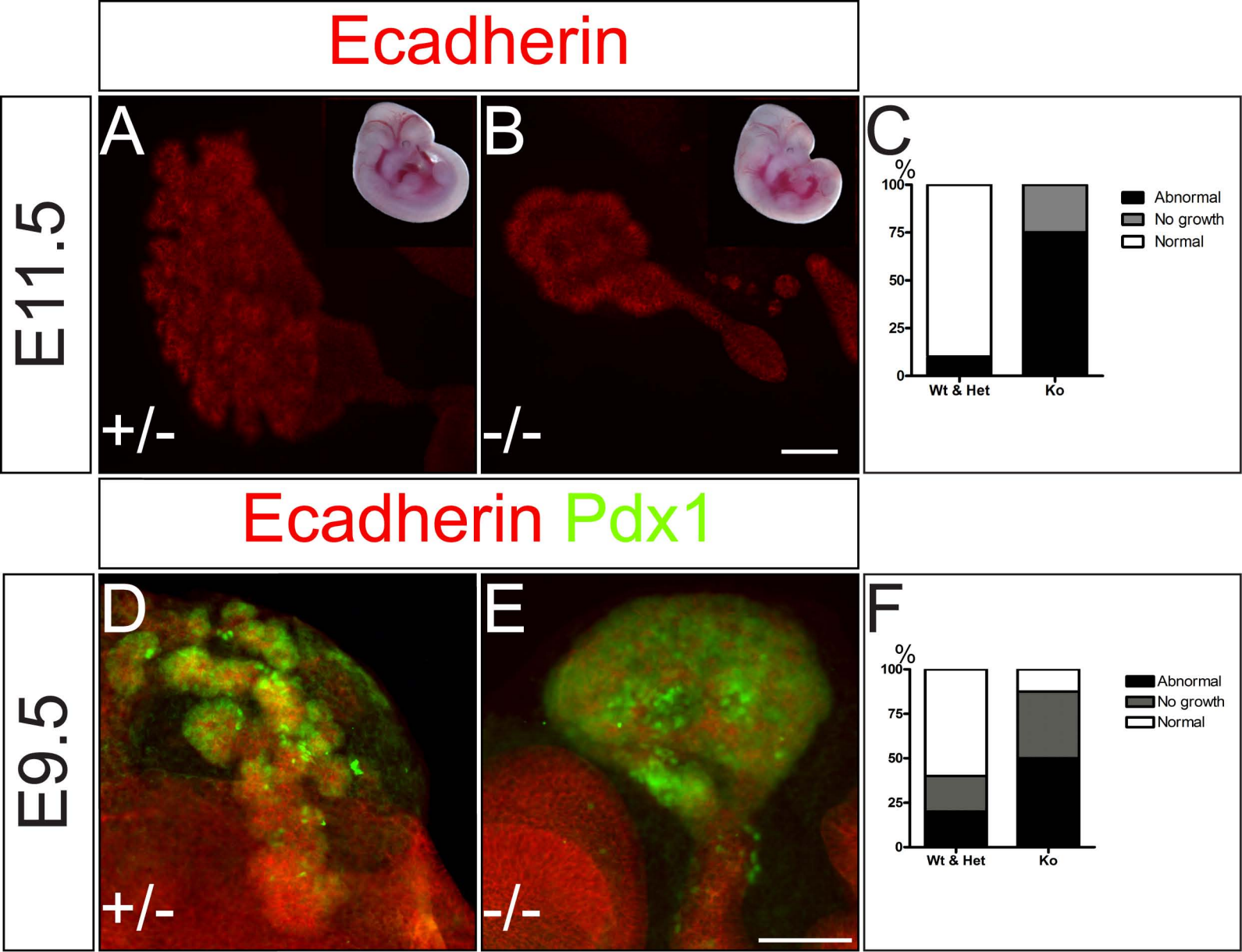
Ecadherin
E11.5
A
+/-
B
-/-
C
%
100
75
50
25
0
Wt & Het
Ko
Abnormal
No growth
Normal
Ecadherin Pdx1
E9.5
D
+/-
E
-/-
F
%
100
75
50
25
0
Wt & Het
Ko
Abnormal
No growth
Normal

Dorsal Pancreas

Pdx1 BrdU

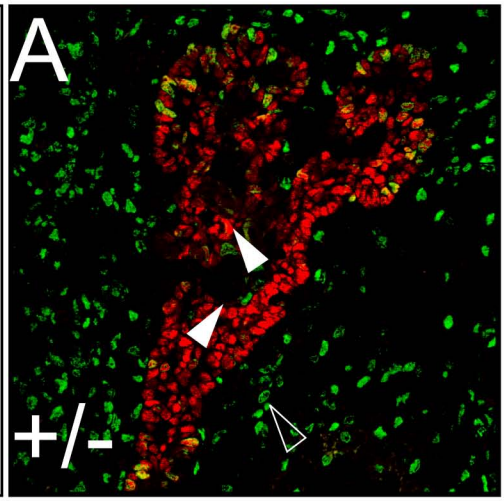

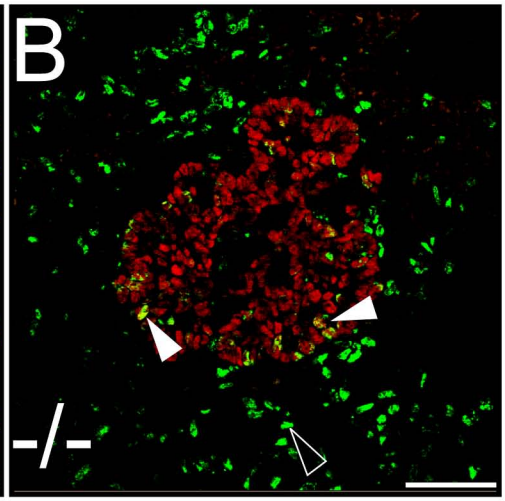

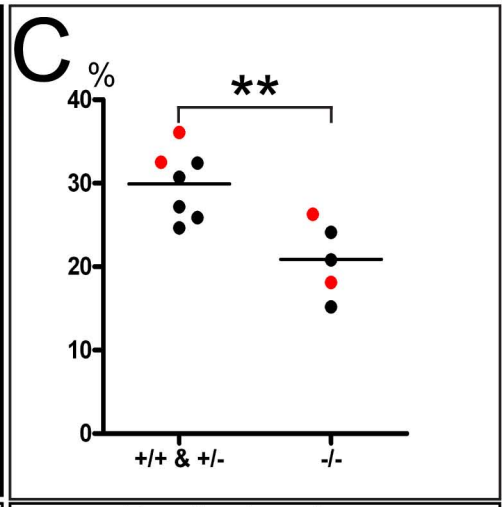

Glu Ecad

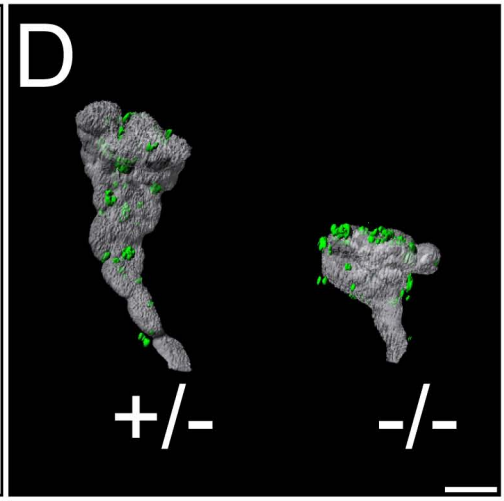

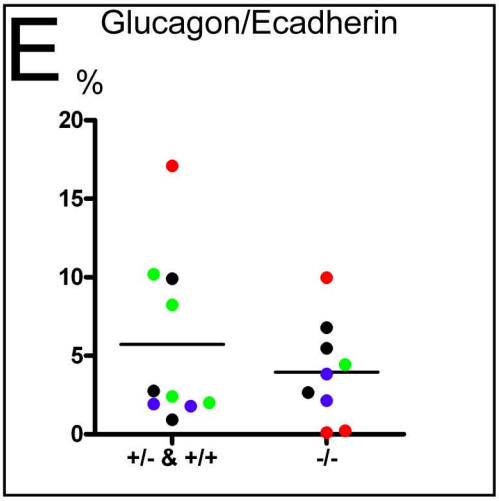

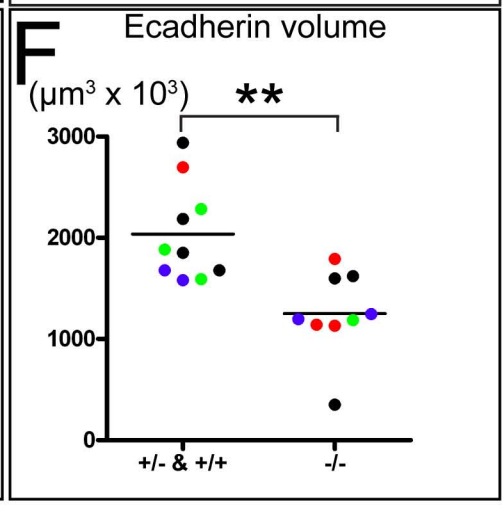

Ins Ecad

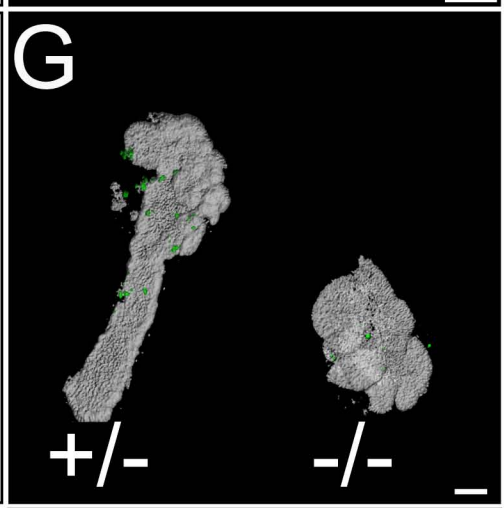

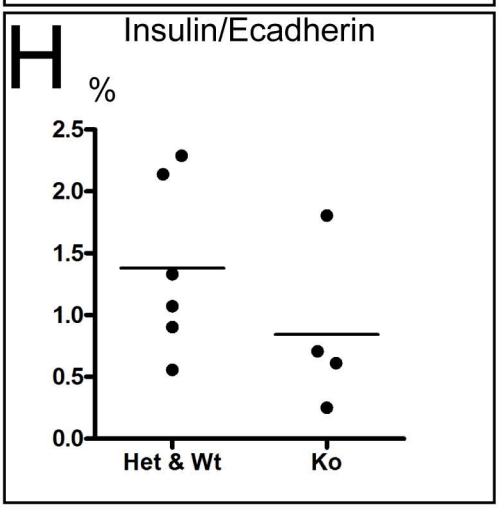

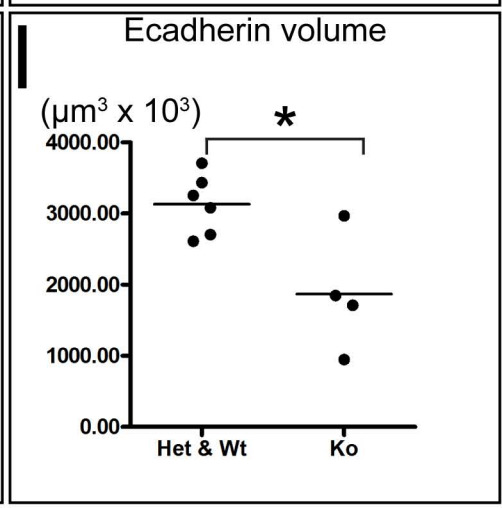

Mucin1

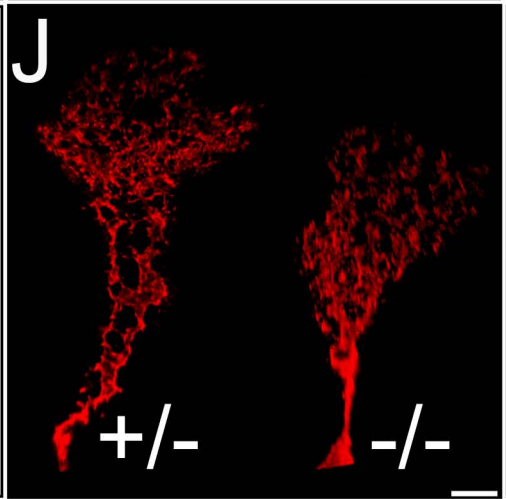

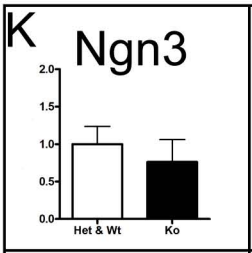

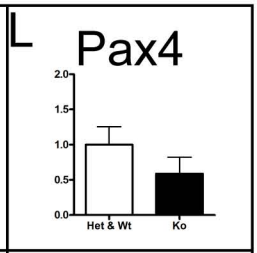

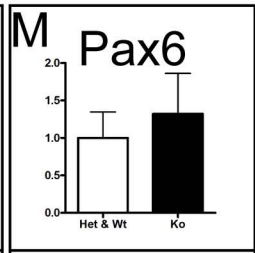

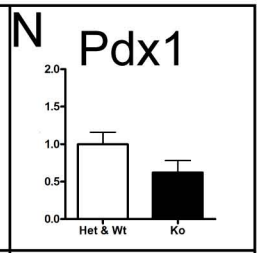

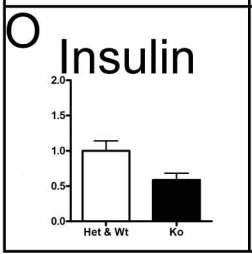

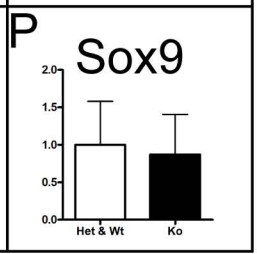

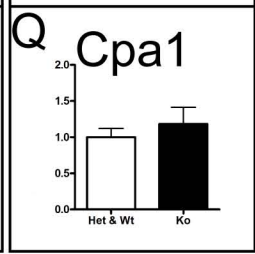

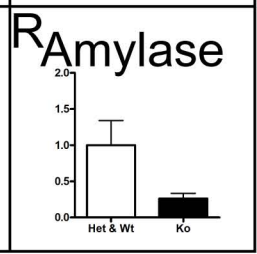

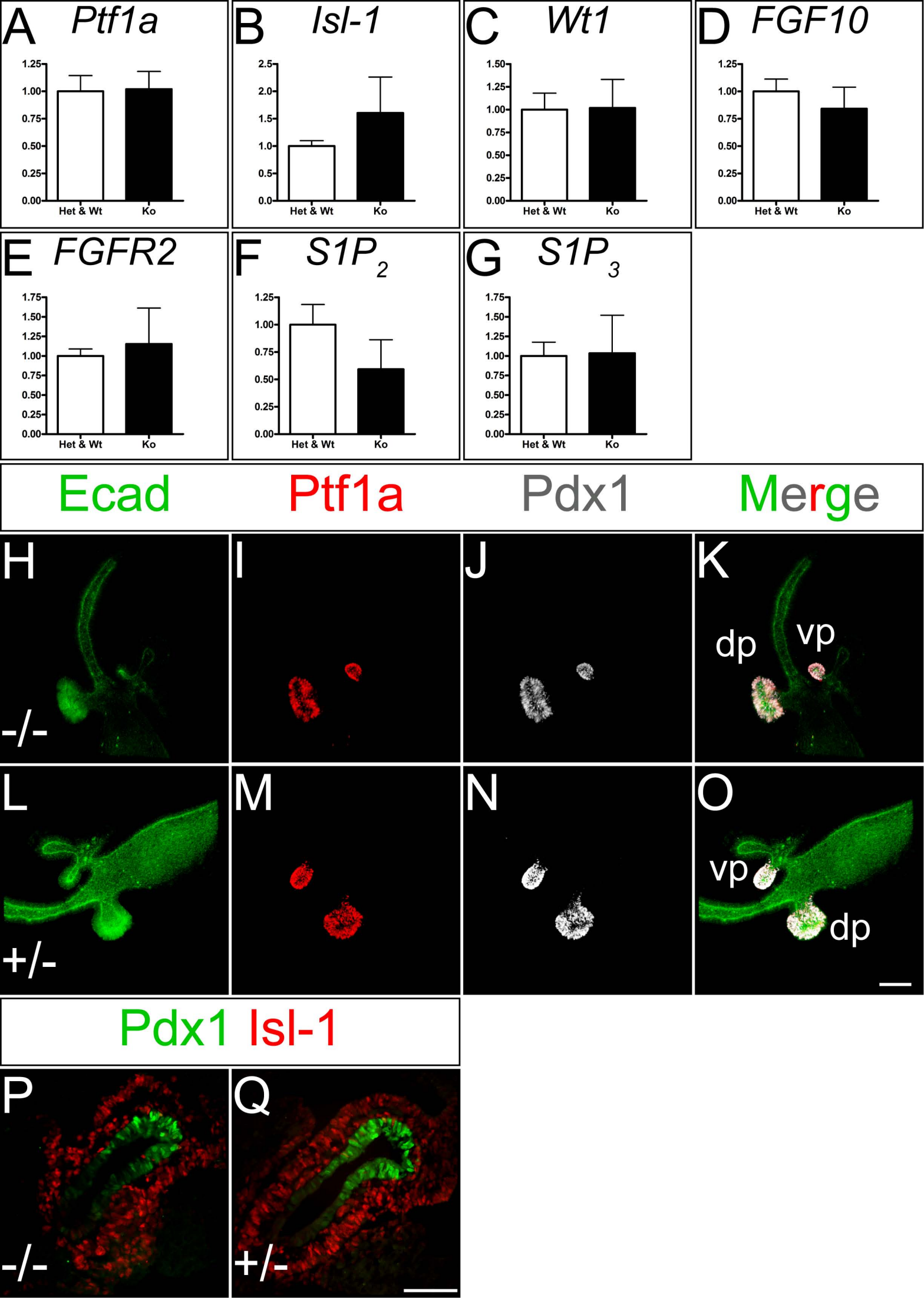
A Ptf1a
B Isl-1
C Wt1
D FGF10
E FGFR2
F S1P2
G S1P3
Het & Wt
Ko
Ecad
Ptf1a
Pdx1
Merge
H
I
J
K
dp
vp
-/-
L
M
N
O
vp
dp
+/-
Pdx1 Isl-1
P
Q
-/-
+/-

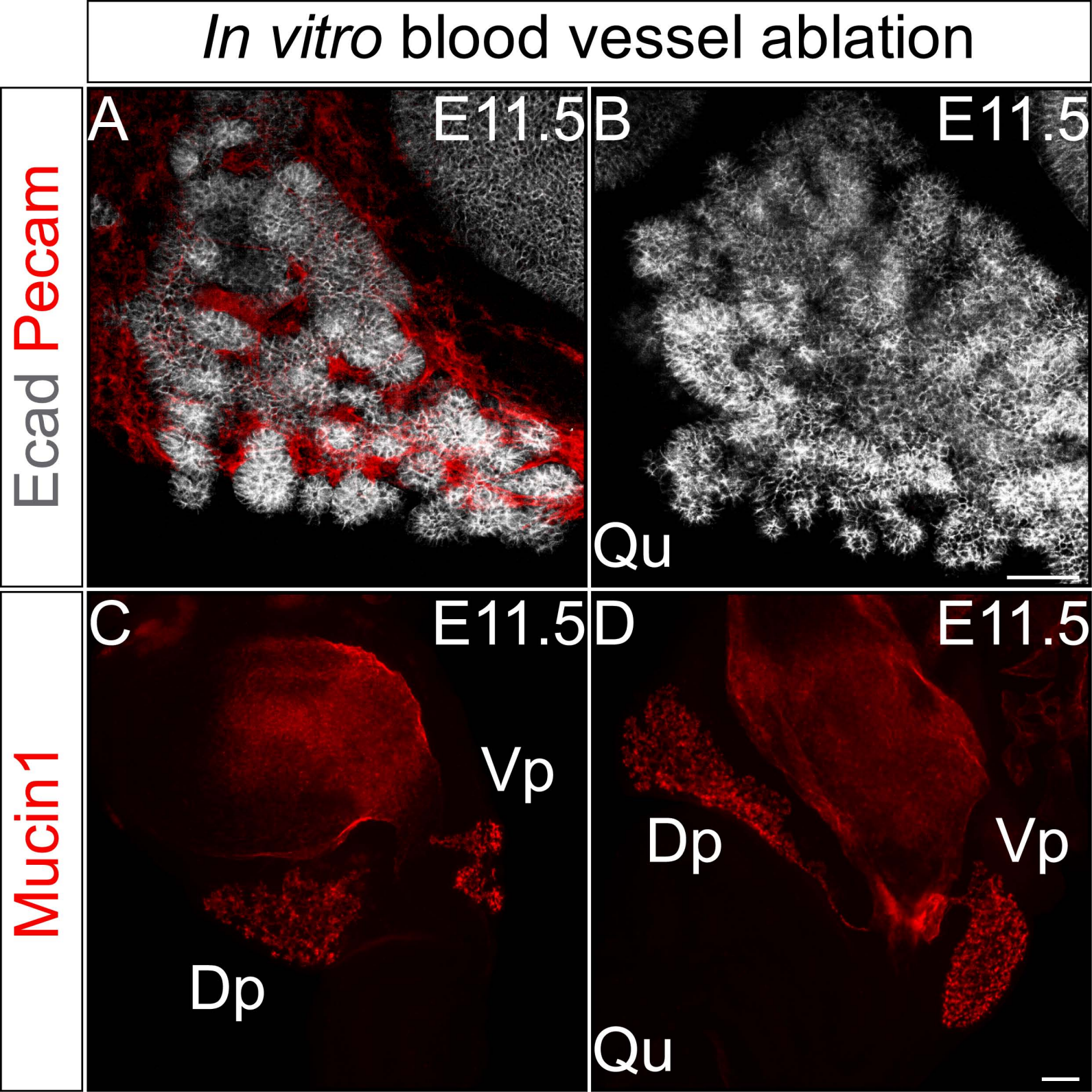
In vitro blood vessel ablation
Ecad Pecam
Mucin1
A
E11.5
B
E11.5
Qu
C
E11.5
Vp
Dp
D
E11.5
Dp
Vp
Qu

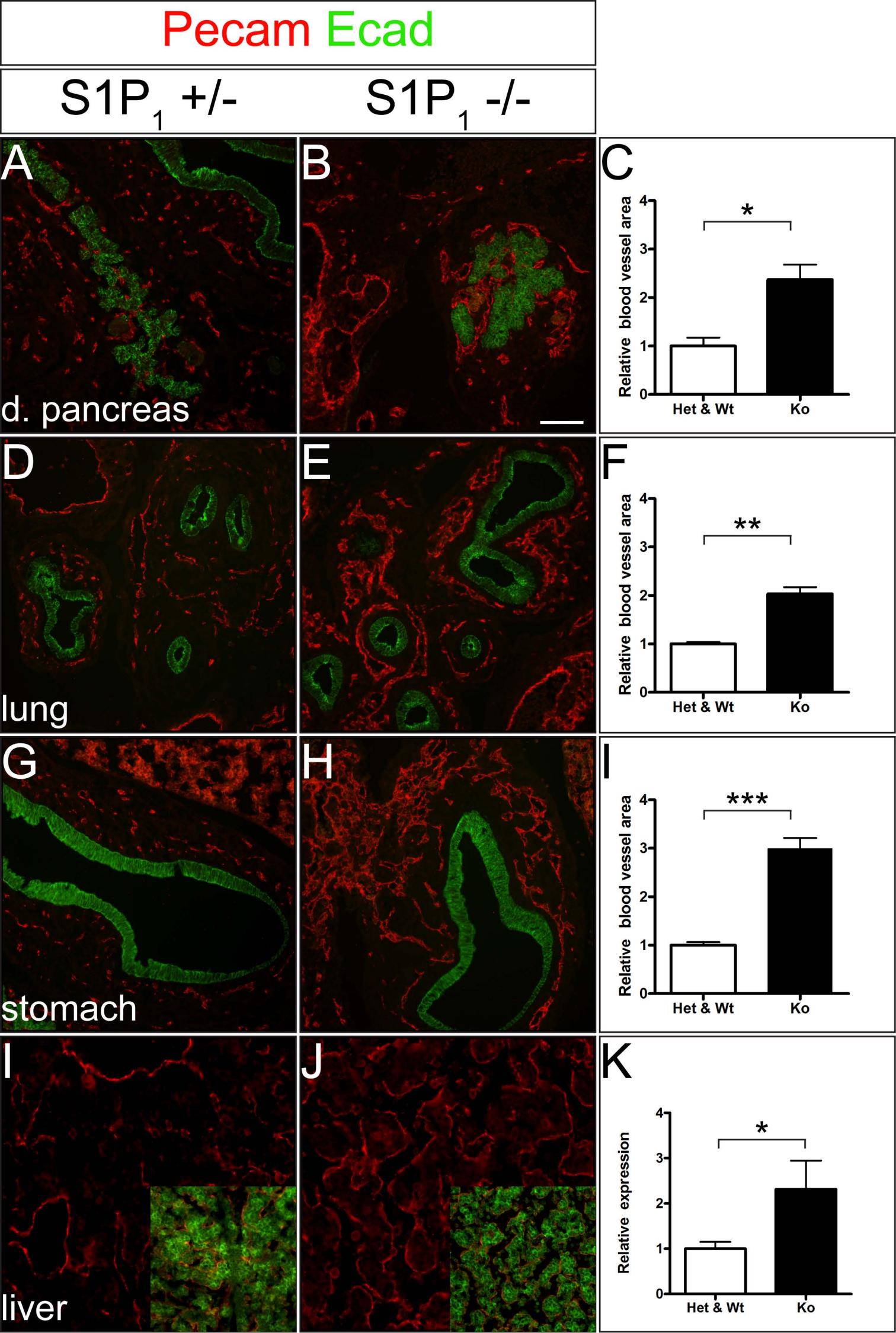
Pecam Ecad
S1P1 +/-
S1P1 -/-
A
B
C
d. pancreas
Relative blood vessel area
*
Het & Wt
Ko
D
E
F
lung
**
G
H
I
stomach
***
I
J
K
liver
Relative expression
*

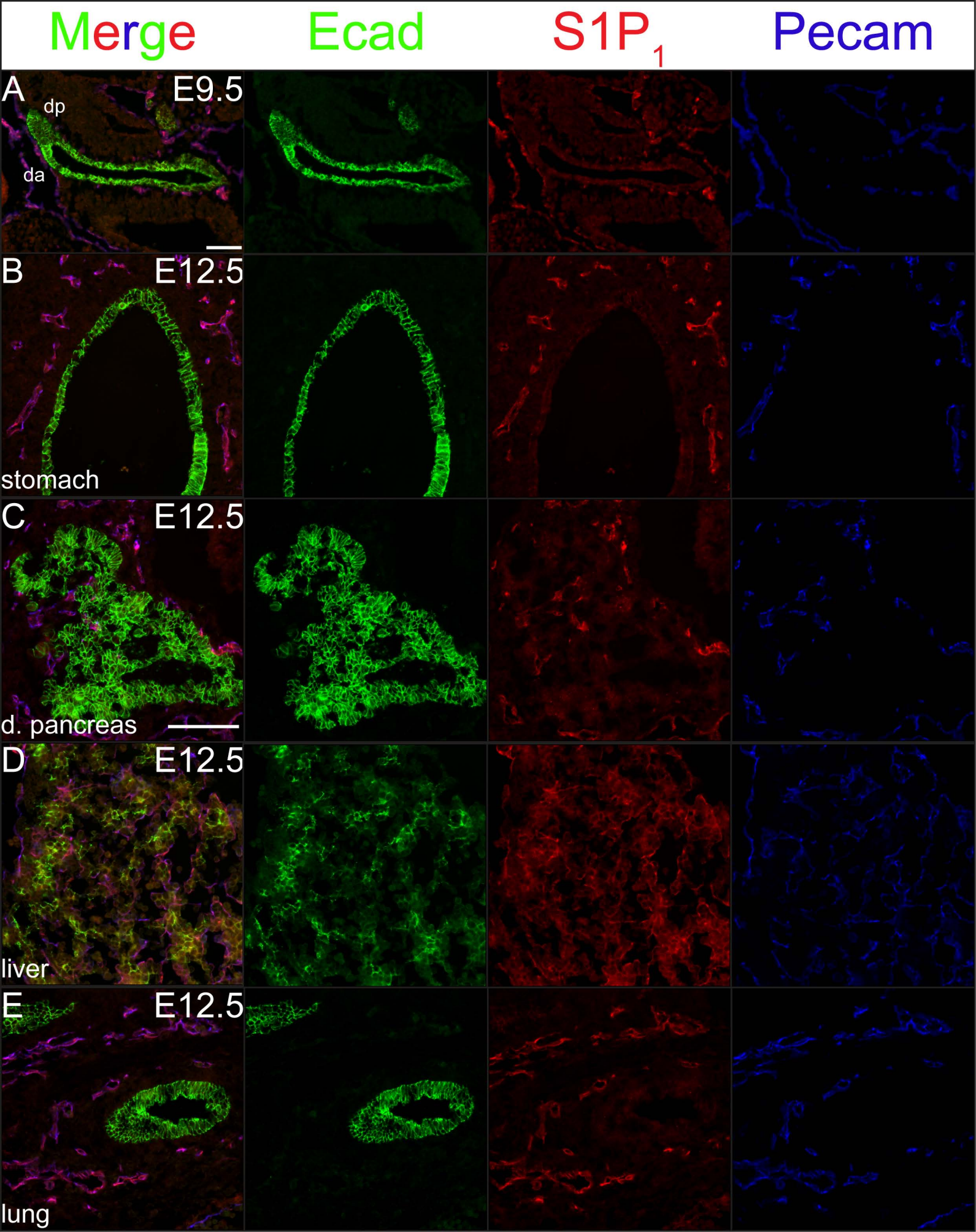
Merge
Ecad
S1P1
Pecam
A
E9.5
dp
da
B
E12.5
stomach
C
E12.5
d. pancreas
D
E12.5
liver
E
E12.5
lung

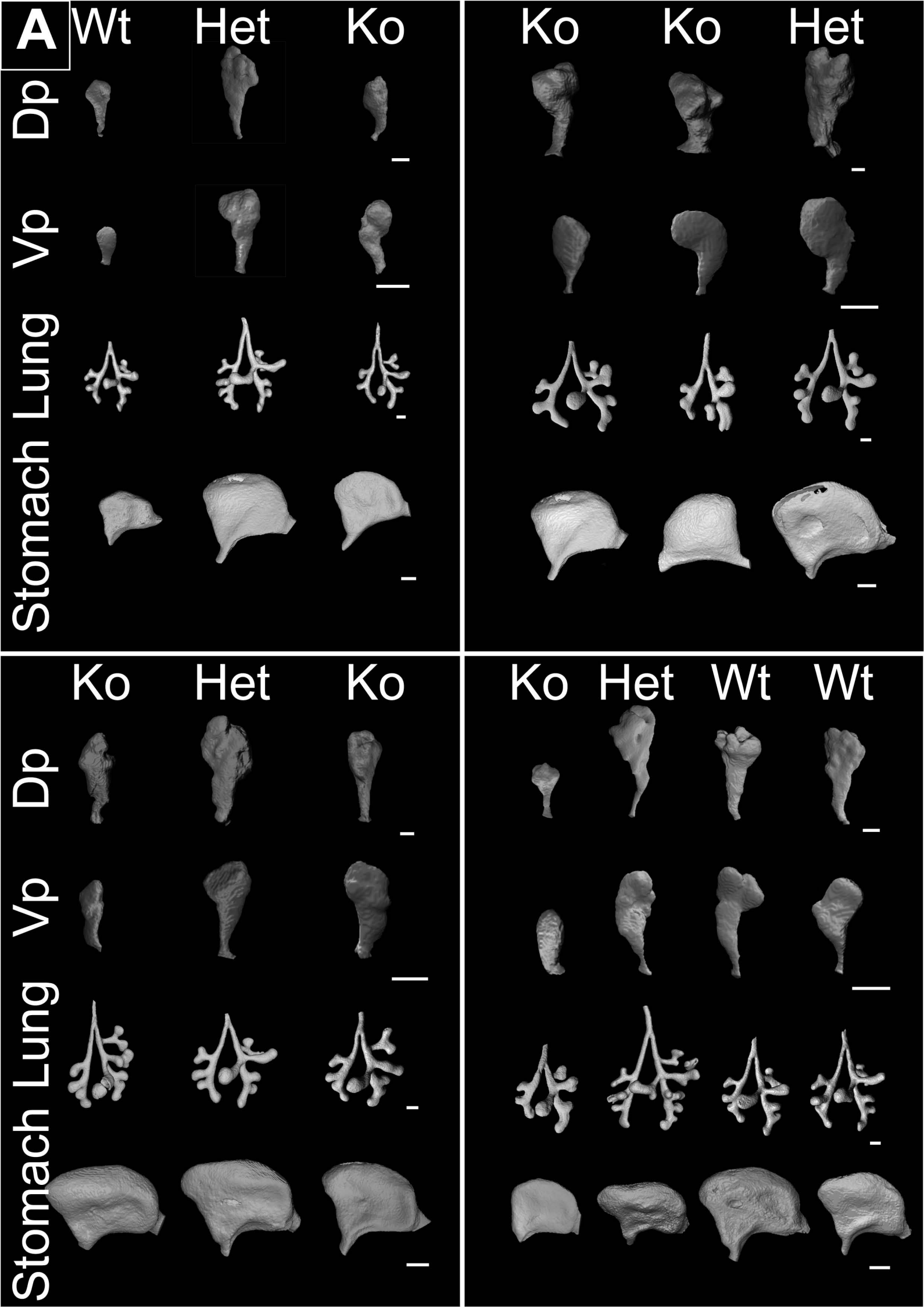
A
Wt
Het
Ko
Ko
Ko
Het
Dp
Vp
Lung
Stomach
Ko
Het
Ko
Ko
Het
Wt
Wt
Dp
Vp
Lung
Stomach

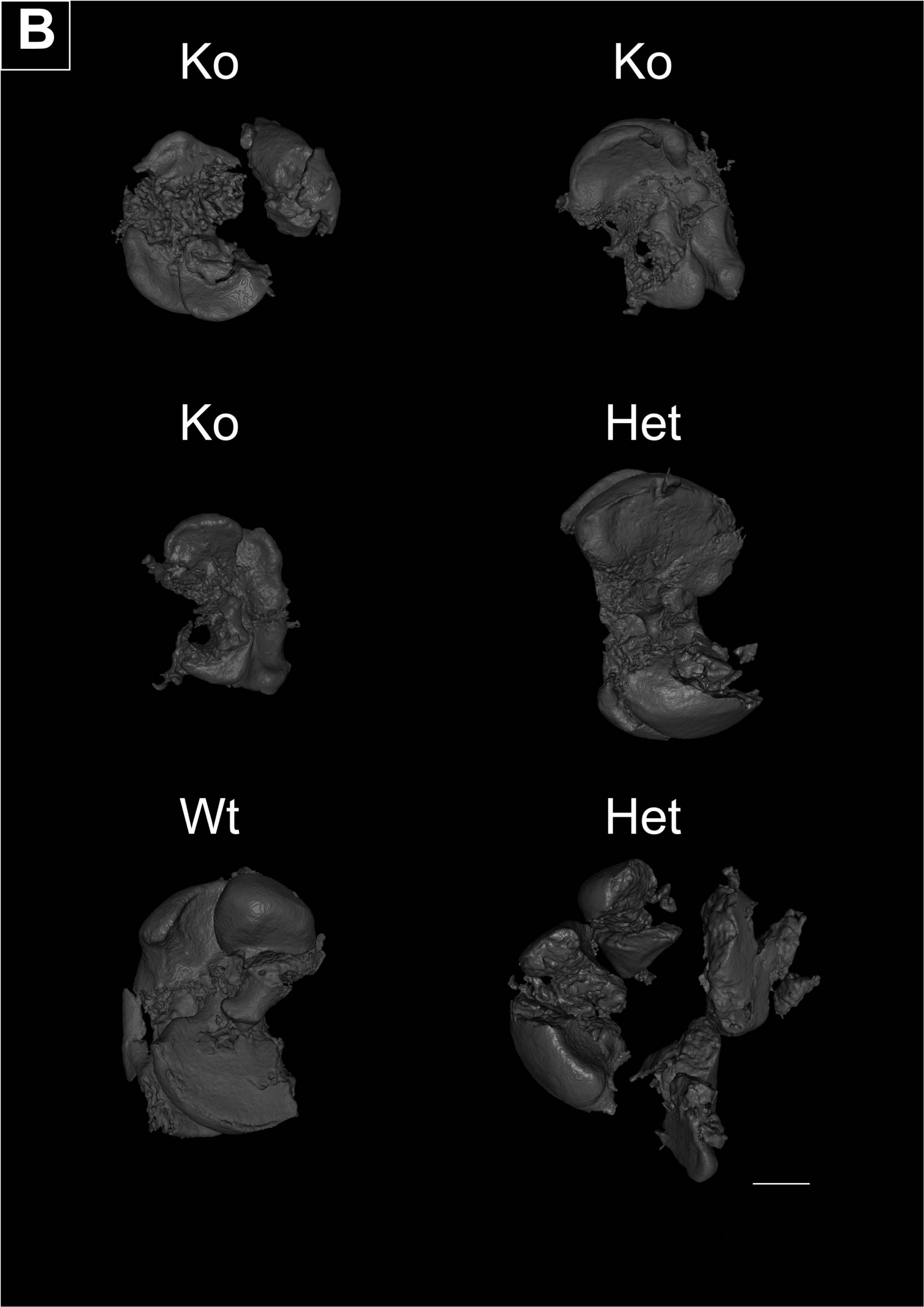
B
Ko
Ko
Ko
Het
Wt
Het

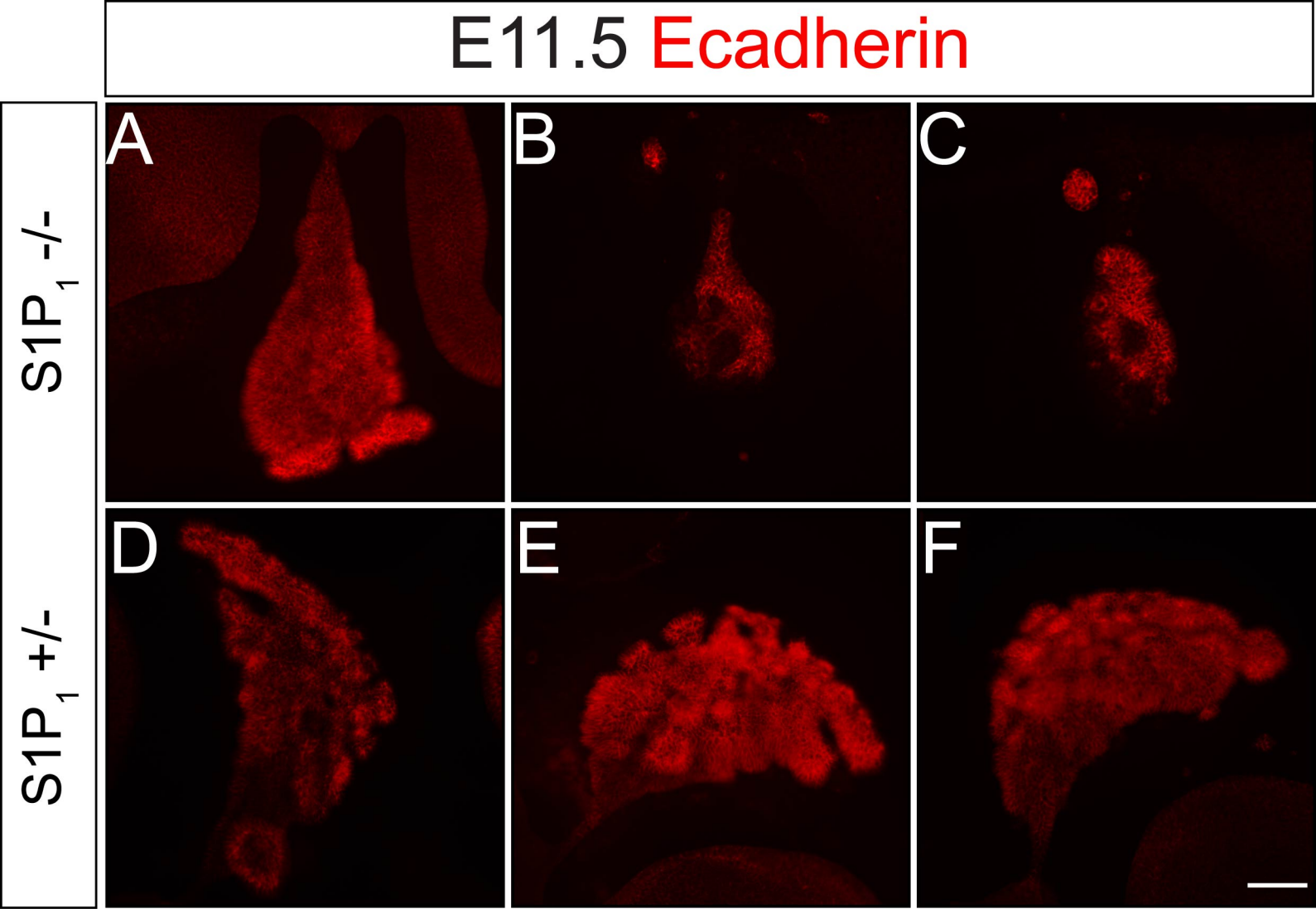
E11.5 Ecadherin
A
B
C
D
E
F
S1P1 -/-
S1P1 +/-

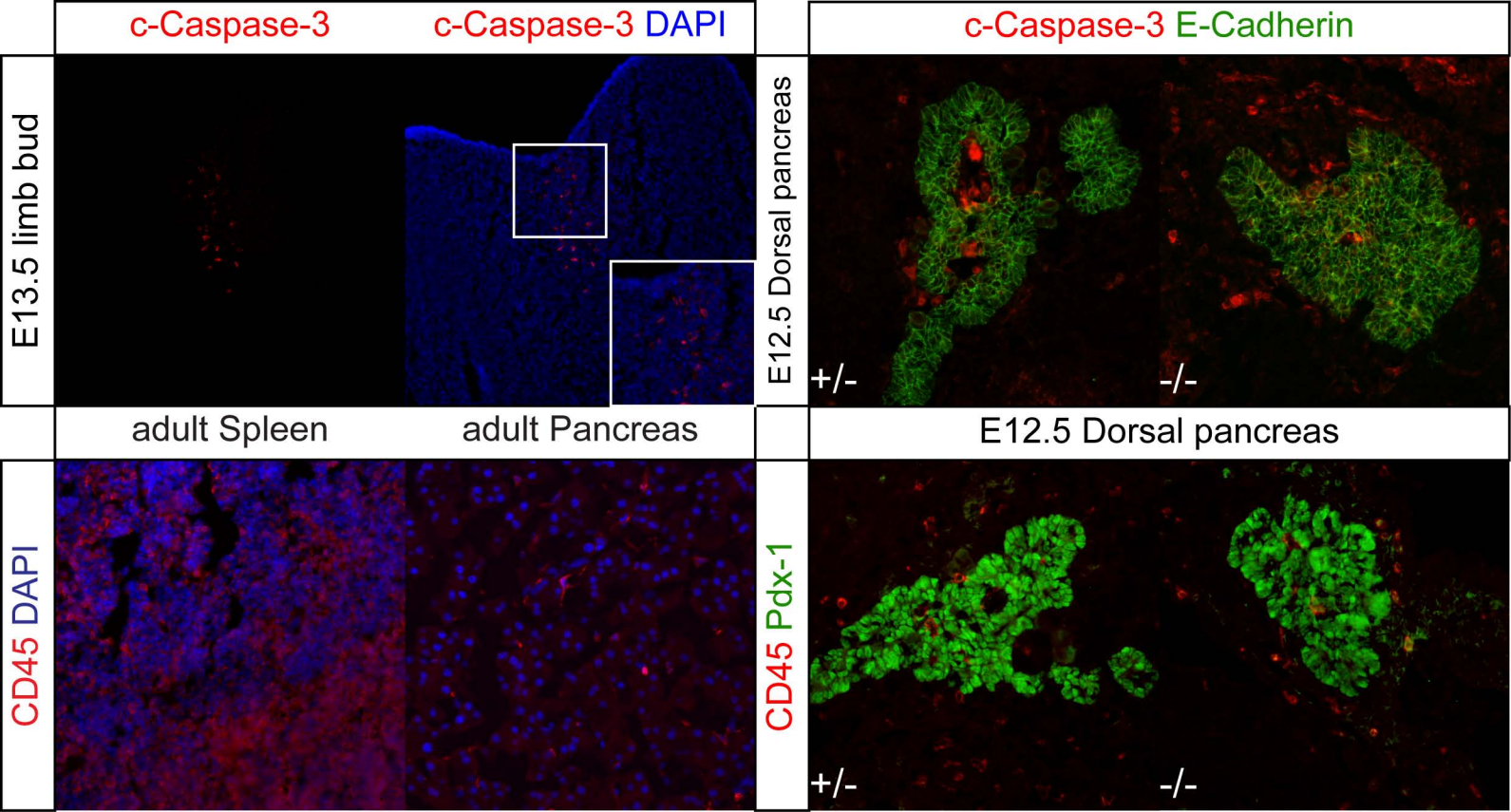
c-Caspase-3
c-Caspase-3 DAPI
E13.5 limb bud
c-Caspase-3 E-Cadherin
E12.5 Dorsal pancreas
+/-
-/-
adult Spleen
adult Pancreas
CD45 DAPI
E12.5 Dorsal pancreas
CD45 Pdx-1
+/-
-/-

Gene	Primer Pair
beta-actin	Mouse Endogenous Control Panel
beta-2-microglobulin	Mouse Endogenous Control Panel
Ptf1a	5’-CTTGCAGGGCACTCTCTTTC-3’ 5’-CGATGTGAGCTGTCTCAGGA-3’
$S1P_2$	5’-CACAGCCAACAGTCTCCAAA-3’ 5’-ATGTCCAGCGTCTCCTTG-3’
$S1P_3$	5’-TAGCGGGAGAGAAACCTGA-3’ 5’-GCGGGAAGAGTGTTGAAAAT-3’
Isl1	5’-AGCAACCCAACGACAAAACT-3’ 5’-AGAGCCTGGTCCTCCTTCTG-3‘
Wt1	5’-GAGAGCCAGCCTACCATCC-3’ 5’-GGGTCCTCGTGTTTGAAGG-3’
FGF10	5’-CCTCGTCCTTCTCCTCTCCT-3’ 5’-TTGCTGTTGATGGCTTTGAC-3’
FGFR2	5’-TACCCTCACAGAGACCCACA-3’ 5’-GAATCGTCCCCTGAAGAACA-3’
Ngn3	5’-TGGCCCATAGATGATGTTCG-3’ 5’-AGAAGGCAGATCACCTTCGTG-3’
Pax4	5’-TGTGCTGGAACCATTGAGTC-3’ 5’-AATGGGTTGATGGCACTTGT-3’
Pax6	5’-AAACAAACGCCCTAGCTCTCC-3’ 5’-CCGCCCTTGGTTAAAGTCTTC-3’
Pdx1	5’-GAAATCCACCAAAGCTCACG-3’ 5’-TTCAACATCACTGCCAGCTC-3’
Insulin	5’-CCCTGCTGGCCCTGCTCTT-3’

	5’-AGGTCTGAAGGTCACCTGCT-3’
Sox9	5’-CCACGGAACAGACTCACATC-3’ 5’-CTGCTCAGTTCACCGATGTC-3’
Cpa1	5’-GACGAGGAGAAGCAGCAGAT-3’ 5’-GATGCCAGTGTCAATCCAGA-3’
Amylase	5’-AGGTCATTGATCTGGGTGGTG-3’ 5’-GACATCTTCTCGCCATTCCAC-3’
HPRT	5’-AGCCCCAAAATGGTTAAGGT-3’ 5’-CAAGGGCATATCCAACAACA-3’

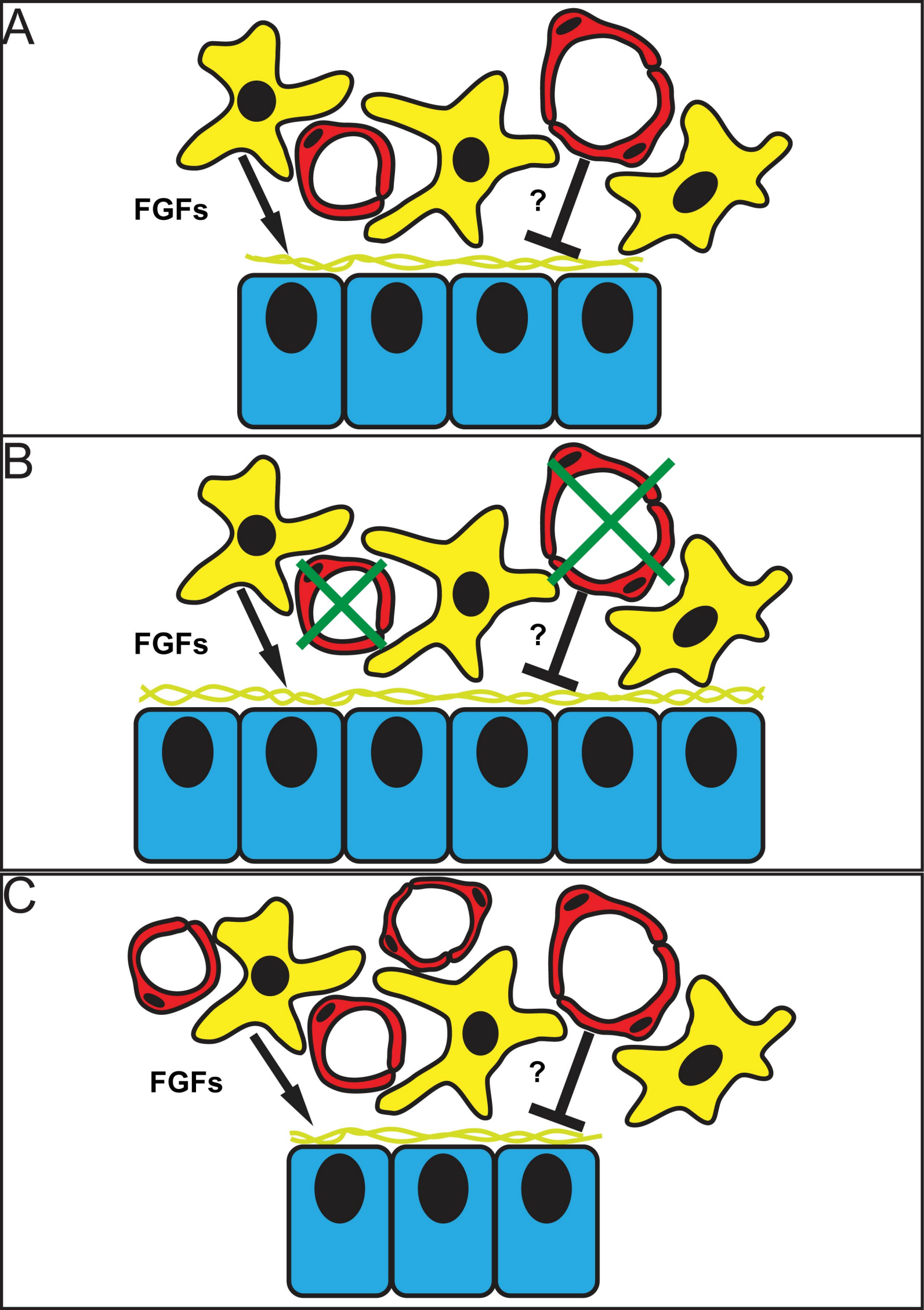
A
FGFs
?
B
FGFs
?
C
FGFs
?